

Diese Arbeit wurde vorgelegt am  
Lehr- und Forschungsgebiet Theorie der hybriden Systeme

**Optimale Platzierung von Windkraftanlagen mit  
unterschiedlicher Nabenhöhe**  
**Optimal Placement of Wind Turbines with Different  
Hub Heights**

Bachelorarbeit  
Informatik

April 2022

Vorgelegt von Presented by	Almut Herzog Matrikelnummer: 398035 almut.herzog@rwth-aachen.de
Erstprüfer First examiner	Prof. Dr. rer. nat. Erika Ábrahám Lehr- und Forschungsgebiet: Theorie der hybriden Systeme RWTH Aachen University
Zweitprüfer Second examiner	Prof. Dr. rer. nat. Thomas Noll Lehr- und Forschungsgebiet: Software Modellierung und Verifikation RWTH Aachen University
Betreuer Supervisor	Dr. rer. nat. Pascal Richter Lehr- und Forschungsgebiet: Theorie der hybriden Systeme RWTH Aachen University

## Eigenständigkeitserklärung

Hiermit versichere ich, dass ich diese Bachelorarbeit selbständig verfasst und keine anderen als die angegebenen Quellen und Hilfsmittel benutzt habe. Die Stellen meiner Arbeit, die dem Wortlaut oder dem Sinn nach anderen Werken entnommen sind, habe ich in jedem Fall unter Angabe der Quelle als Entlehnung kenntlich gemacht. Dasselbe gilt sinngemäß für Tabellen und Abbildungen. Diese Arbeit hat in dieser oder einer ähnlichen Form noch nicht im Rahmen einer anderen Prüfung vorgelegen.

Aachen, im April 2022

Almut Herzog

# Contents

<b>1. Introduction</b>	<b>1</b>
1.1. Related Work . . . . .	2
1.2. Contribution . . . . .	5
1.3. Outline . . . . .	6
<b>2. Potential Area</b>	<b>6</b>
2.1. Distances to Objects . . . . .	6
2.2. Algorithm . . . . .	8
<b>3. Energy Yield Forecast</b>	<b>13</b>
3.1. Regional Wind Data . . . . .	13
3.2. Annual Energy Production . . . . .	16
3.3. PARK Turbulence Model . . . . .	17
3.4. Levelized Cost of Energy . . . . .	18
<b>4. Optimal Positioning</b>	<b>20</b>
4.1. Optimal Positioning of Wind Turbines with One Clearly Defined Hub Height . . . . .	21
4.1.1. Ellipse-Based Algorithm . . . . .	21
4.1.2. Refinement Step . . . . .	23
4.2. Optimal Positioning of Wind Turbines with Different Hub Heights . . . . .	24
4.2.1. Greedy Algorithm . . . . .	25
4.2.2. Refinement Step . . . . .	26
<b>5. Case Study</b>	<b>26</b>
5.1. Potential Area . . . . .	27
5.2. Optimal Positioning and Energy Yield Forecast . . . . .	28
5.3. Discussion of Results . . . . .	29
<b>6. Conclusion and Future Work</b>	<b>34</b>
6.1. Future Work . . . . .	35
<b>A. Turbine Properties</b>	<b>36</b>
<b>B. Plots</b>	<b>37</b>
B.1. Plots of Exemplary Ellipse-Based Optimization . . . . .	37
B.2. Plots of Potential Area . . . . .	46
B.3. Plots of Final Turbine Positioning . . . . .	48
B.3.1. Ellipse-Based Algorithm . . . . .	48
B.3.2. Greedy Algorithm . . . . .	53
<b>References</b>	<b>58</b>

# 1. Introduction

There are numerous reasons and impulses to deal more with approaches to the production of renewable energies: In addition to the most recent reasons relating to the Russian war of aggression in Ukraine, people living in Germany have also been preoccupied for some time with the rapidly rising electricity and gas prices since the beginning of 2021, the still unsolved problem around the storage of radioactive waste from nuclear power plants, the damage caused by and the shrinking of deposits of oil and natural gas, to name just a few.

People are responsible for their environment. This is why the issue of climate protection must be addressed more emphatically. For this reason, greater emphasis is to be placed on renewable energies and this leads to research about optimizing such forms of energy generation.

An additional task is to increase acceptance in parts of the population for the design of new energy plants in their neighborhood. Some scientists are confident that they could help to overcome these reservations by providing better information about the actual conditions of such plants.

One hope for sustainable energy production is the use of wind farms.

An important approach to optimizing the generation of electrical energy by wind turbines is to arrange several wind turbines in one area.

How a wind turbine is constructed can be taken from Figure 1: Wind turbines generate electrical power by the kinetic energy from the flow of wind hitting the rotor blades as normal as possible setting the wind turbine in motion. This mechanical rotational energy is transferred by a shaft, which in turn is connected to the generator. There, a coil rotates accordingly, ultimately generating electrical energy.

A gearbox is usually placed in front of the generator, which converts the rotational speed of the rotor into faster rotational speeds of the coil in the generator. The generator is connected to the power grid through the tower.

However, problems can arise in this process. Above a certain density of the wind turbines, their energy production is impaired: Due to the rotation of the rotors, the wind flow becomes highly three-dimensional above a certain speed. This means that larger wind eddies form in the wind stream behind the turbine than would normally be expected from the ground-level atmospheric flow. With increasing distance, the size of the eddies decreases, which is why, after a certain distance, there is again almost no disturbance in the wind flow, as mentioned by Hahm [27].

The phenomenon that occurs is called wake. Due to the turbulence generated by the rotation of the wind turbines, neighboring wind turbines can then no longer convert the wind energy reaching them into electrical energy as efficiently as if there was no wake affecting them. For this to happen, the wind flow would have to be as laminar as possible.

The undesired influence of these effects can be reduced by planning wind turbines with different heights and rotor diameters on one area. The different heights allow various optimizations to be made, such as reducing the distances between wind turbines while

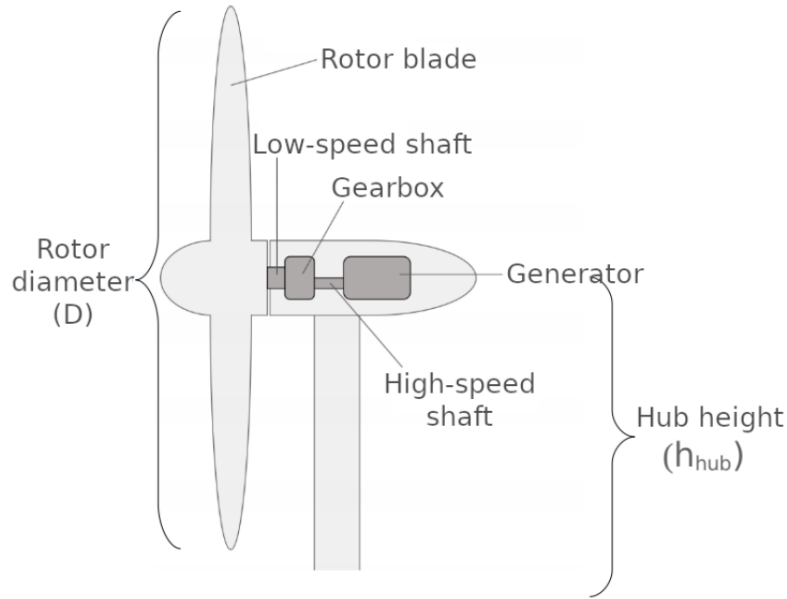


Figure 1: Construction of a wind turbine. The components important for power generation are shown from the side [59]. The total height  $H$  can be calculated by adding the hub height  $h_{\text{hub}}$  and half the rotor diameter  $D$ .

maintaining the same efficiency, or higher expectation of energy output.

## 1.1. Related Work

In particular, this work revolves around the Wind Farm Layout Optimization Problem (WFLOP). An objective for this would be to maximize the electrical energy generated by a wind farm while minimizing the costs. For this purpose, the wind turbines should be optimally positioned in the wind farm so that the wake loss is as low as possible. The goal is therefore the maximum expected power production at the minimum cost of energy; the unit generally chosen here is the cost in Euros per megawatt hour (€/MWh).

There is literature that also deals with other factors, such as design or logistical issues, for example, in Samorani [48].

Furthermore, there is a lot of work on compensating or considering certain difficulties when performing optimization approaches. For example, physical properties are considered, such as naturally occurring turbulence in the lower part of the Earth's atmosphere due to ground friction and heating, as Calaf et al. [5] describe. Considering turbines as a roughness element in this layer is studied, for example, by Frandsen [22]. A widely used strategy to simulate atmospheric stability conditions is the Park wake model that will be explained later in Section 3.3 developed by Jensen [32] and Katic et al. [49, 33]. It generally shows good agreement with real collected data, as can be read in Peña [46] and by de Barros Neiva et al. [41] in a review.

Among others, Sørensen et al. [55] established that this model withstands well to

comparison with other wake models for specific offshore wind farms. This conclusion was also reached by Shakoor et al. [52], who also investigated different wake models for simplicity and accuracy.

Responsible for wake losses are, as already mentioned, the distances between wind turbines. There is also a lot of literature on the optimal spacing of wind turbines. For example, Khanali et al. [34] describe why the longitudinal distance between turbines should be reasonably larger than their latitudinal distance. In Germany, the so-called  $3D/5D$  rule is often used<sup>1</sup>. This is the abbreviation for the widely implemented spacing regulation between wind turbines of five rotor diameters in the main wind direction and three rotor diameters orthogonal to it, which will be later explained in more detail, see Section 4.1.

The most used approach to prepare the area of the considered region for the application of an optimization approach is to divide it into a grid. From Wang et al. [57], for example, there is a paper on parameters such as shape, direction, and density of grid cells. In contrast, there are also works without the use of a grid, for example by Moorthy et al. [39], where turbines are positioned in a radius of 200 meters away from all others.

However, many optimization approaches only consider contiguous, usually rectangular surfaces in theory, which is not often found in reality. Gu et al. [25], for example, present two methods of dealing with this problem in their paper and then also show the effectiveness of their approaches using real existing wind farms.

Another problem with the area is that landowners often need to be considered in planning, and their interests do not necessarily coincide with those of the initiators. To facilitate this, Chen et al. [10] present a guide by identifying the most important positions for wind turbines on a site. This makes it clear which landowners should be particularly persuaded to give the go-ahead to build wind turbines.

For the solution of the WFLOP, there are now numerous approaches and for the majority of these, there are in turn many improvement strategies or reviews. A general overview can be found for example in González et al. [51], where different state-of-the-art solutions for wind farm optimization are explained for different target parameters and local conditions. Most of the solutions can be divided into mathematical and biological optimization approaches.

One mathematical and statistical method, for example, is Monte Carlo simulation, which is used by Marmidis et al. [38]. Matching this is the particle filtering approach, which is covered by Eroğlu et al. [20], which also shows that this approach can certainly compete with others derived from biology. Another effective solution technique compared to other state-of-the-art methods is using meta-heuristics algorithms based on basic teaching-learning optimization algorithms, described by Patel et al. [45].

Other approaches extend pattern search algorithms: Various approaches can be found,

---

<sup>1</sup>Overview onshore wind energy, 2019 [https://www.fachagentur-windenergie.de/fileadmin/files/Veroeffentlichungen/Faktenpapiere/FA\\_Wind\\_Hoehenbegrenzungen\\_Wind-an-Land\\_03-2019.pdf](https://www.fachagentur-windenergie.de/fileadmin/files/Veroeffentlichungen/Faktenpapiere/FA_Wind_Hoehenbegrenzungen_Wind-an-Land_03-2019.pdf). Accessed 24 Apr 2022.

some of them discussed by DuPont et al. [15, 17, 16], for example.

Many solutions, in particular, look for models in biology: There are evolutionary algorithms by Rodrigues et al. [47] or González et al. [53], but also multi-step combinations with other optimization algorithms, as described in Shin et al. [53], for example.

Some propositions are based on particle swarm optimization, such as Luo et al. [37], Chowdhury et al. [14], or Hou et al. [30], in each of which the focus is on different constraints. Long et al. [36] have developed a multi-step algorithm also including particle swarm optimization that can outperform other approaches.

Another approach derived from biology is biogeography-based optimization, for example by Nagar et al. [3], viral-based optimization algorithms, such as by Dagli et al. [31], or ant colony algorithms, such as those considered by Eroğlu et al. [19] considered.

However, a particularly large amount of work relates to solution strategies using the genetic algorithm, as this has proven to be a good optimization approach in electric power systems, especially under multi-objective methods. Interesting work on this has been done, for example, by Grady et al. [24], Parada et al. [43], Ogunjuyigbe et al. [42], Park et al. [44], and Gatscha [23]. Again depending on the work, the focus was additionally on various other properties.

The genetic algorithm is also often used to optimize individual wind turbine components, see Ammous et al. [1], Selig et al. [50], or a comparison by Song et al. [54] with also particle swarm optimization used.

Finally, there are greedy solution strategies. Repeated adaptations can create an approach that may be better than others. Suggestions are given, for example, by Chen et al. [7] and Ozturk et al. [2].

Some of the sources mentioned already address different hub heights or rotor diameters of the proposed wind turbines. While there is an article by Chen et al. [8] on determining the optimal height of wind turbines on a specific area, it must be noted that whenever this is investigated, it turns out that the respective optimization results regarding economic values of wind farms can be further improved by different heights. Evidence can be found in the following, among others: Chen et al. find, both for optimization by the genetic algorithm [11], and for optimization with a greedy algorithm [9], that even for the same number of turbines, varying heights can increase the power and decrease the cost per unit power. Thereby, the results of the greedy approach can even surpass those of the genetic algorithm. Chowdhury et al. [13] explain in their work on unrestricted wind farm layout optimization simultaneously the best wind farm layout and the best turbine selection based on their rotor diameter. They find that differing rotor diameters lead to higher efficiency and better cost allocation. By Chowdhury et al. [12] there is also a paper that uses particle swarm optimization to find that different rotor diameters play an important role in the efficiency of a wind farm. Also, Mustakerov et al. [40] investigate an approach to combinatorial optimization for wind turbine types, as well as their number and positioning under different conditions. Furthermore, there are observations of Vassel-Be-Hagh et al. [56], who present optimization by only adjusting the turbine height, leaving all other properties unchanged in each case. Repeatedly, alternating hub heights are found to lead

to better results.

Overall, it is also noticeable that there is more literature on offshore wind farms than on onshore wind farms. This is certainly mainly due to the fact that there is more wind offshore with less turbulence at the same time since it can flow more freely. In addition, less attention must be paid to topographical difficulties such as complex terrain and sometimes large differences in altitude. Göçmen et al. [26] present a comparison of different wake models for onshore and offshore wind farms.

In general, new works on wind farm optimization are published all the time, so new knowledge is constantly being gained. A very broad overview of this can be found in Herbert-Acero et al. [29], where literature and models on WFLOP are collected and classified in general. However, this can certainly be updated again, for example, recent research suggests that possibly the wind turbine design should be completely rethought. Instead of a horizontal axis a vertical one should be chosen, as described among others by Whittlesey [58]. Then, of course, all the guidelines and recommendations would have to be reexamined and reconsidered.

## 1.2. Contribution

This thesis is intended to address an area that has been little considered by previous work: Using a multi-step algorithm, an optimal layout for a wind farm is calculated, taking into account the position of each wind turbine, the topography, and the distances to certain objects.

The special feature is that besides these factors, the possibility to install different available turbine types in a wind farm is included in order to optimize the results of power output and costs. So on one area, if it contributes to the optimization, turbines with different heights and rotor diameters can be planned.

For this purpose, I will present a multi-step ellipse-based procedure for optimizing wind turbines of the same, predefined type on an area, with local refinement. I will adapt this to the situation where all wind turbines in the area have the same properties, but these are not fixed a priori. Furthermore, I will present a greedy algorithm for optimal positioning of wind turbines that are allowed to vary in height and rotor diameter within the region under consideration. For this positioning of wind turbines of different types, an objective function is applied in the greedy algorithm. Here I will try to optimize the cost in relation to the energy output.

The concepts will be shown and interpreted for a real existing region.

Herzogenrath was chosen for this purpose because the work presented is part of an app under development whose test regions are Herzogenrath and Soest. The goal of the app is to provide low-threshold information about new possible wind farms in their direct neighborhood.

All processes described in the following sections are implemented for the app. This is done in the Python programming language.

Accordingly, all runtimes mentioned in the following always refer to the execution of the respective individual programs. Each chapter corresponds to a program of the

modular app. It was tested under the Linux operating system on a 2018's standard notebook.

Consequently, whenever users are mentioned, a user of the respective piece of software and, in the long run, of the app is meant. In other words, every person who runs the software.

### **1.3. Outline**

In order to document the procedure for this task, it is first necessary to describe conditions for wind farm planning. For this purpose, in Section 2 I explain what distances wind turbines should have to surrounding objects and, as a result, what areas of a region remain free for planning wind turbines.

Subsequently, in Section 3 I explain how the expected levelized cost of electricity can be calculated. This is then an indicator of the optimality of a development plan for a wind farm. Therefore, I also present a model that can be used to calculate the interference of wind turbines with other wind turbines.

In Section 4, the considerations on optimal positioning itself will be described. I will first discuss a way to optimize the positioning of wind turbines of one type and how to make this process as efficient as possible.

The second part of this section is then dedicated to the procedure to find an optimal layout for turbines of different types, including a comparison with the first part.

The considerations are then made illustrative, with a case study in Section 5. This is done by simulations for Herzogenrath in North Rhine-Westphalia (Germany) with the classification of the data obtained in the context of the presented algorithms.

Finally, I will summarize the main statements and results of this work, as well as point out the resulting tasks and perspectives.

## **2. Potential Area**

There are recommendations and restrictions to be observed with regard to distances of wind turbines and wind farms from each other, as well as from certain objects. For this purpose, an overview is given here.

Distances from objects of infrastructure, measuring stations, and certain installations of the military or the federal government, areas for the organization of leisure and recreation are regulated. Furthermore, parts of nature for its protection and the protection of certain species living in it.

Besides, in some federal states, properties such as the size of wind farms or their distances from each other are also determined.

### **2.1. Distances to Objects**

Since in Germany many things are regulated on the level of the federal states, there are many different rules to follow depending on the state: It is regulated by the re-

spective state government how far wind turbines have to be away from certain objects. Additionally, the implementation can vary between specific local areas.

The regulations are also always subject to change, as this is currently a topic of great interest, as can be seen from the introduction (Section 1).

It should also be noted that some terms are interpreted differently locally.

Some rules appear in several federal states, but there are also always certain differences in dealing with the construction of wind farms. Furthermore, one can see that often fixed distances are required, but sometimes the distance from certain objects is made dependent on the height of the planned wind turbine.

Regularly updated information can be found on the website of the associated specialized agency<sup>2</sup>.

In this work, distance regulations for the city-states of Berlin, Bremen, and Hamburg are neglected because these are very densely built-up and do not currently justify the effort.

In the following, I will use the abbreviations  $H$  and  $D$  for the total height of the wind turbine and its rotor diameter according to Figure 1 in Section 1.

From general and purely residential areas there is usually a distance requirement of at least  $2H$  up to 1000 meters, while for detached houses and scattered housing the distance from which the construction of wind turbines is allowed is also in this range but both are often decided on a case-by-case basis and in some cases also depending on policies at the local level. In some places, wind turbines within residential neighborhoods are permitted on a case-by-case basis, too.

Distances to certain facilities in the context of tourism, leisure and recreation zones, camping, as well as spa and hospital areas can vary widely even within many states, from  $2H$  to 6000 meters. Often it is decided depending on each individual case.

In the vicinity of military and defense installations, decisions are usually made on a case-by-case basis. The installations themselves are often protected areas, where no construction is allowed.

For radar stations and measuring stations for earthquakes or by the German meteorological service *Deutscher Wetterdienst (DWD)*, distance rules of up to 10 kilometers apply, but in many places, decisions are again made on a case-by-case basis and sometimes also dependent on the turbine size.

Distances of 20 to 500 meters must be maintained from infrastructure objects such as roads, places of/for air traffic, railway lines, but also overhead power lines, raw material protection, and commercial and industrial areas. This is occasionally specified individually and is also dependent on  $D$ , especially for overhead power lines.

300 to 6000 meters distance must be kept to habitats and breeding areas of various birds and bats, depending on the species. For *Special Protection Areas (SPA)*<sup>3</sup> for

---

<sup>2</sup>Wind energy-relevant information from the federal states <https://www.fachagentur-windenergie.de/veroeffentlichungen/laenderinformationen/laenderinformationen-zur-windenergie/>. Accessed 24 Apr 2022.

<sup>3</sup>Information on Special Protection Areas in Germany <https://biodiversity.europa.eu/countries/germany>. Accessed 24 Apr 2022.

birds, distance regulations of 300 to 700 meters apply depending on the federal state. Around national and nature parks, nature and biosphere reserves, protected forests and biotopes, as well as open space with protection requirement and areas according to the *Habitats Directive*<sup>4</sup> distances of 200 to 1000 meters have to be kept, depending on the case.

For cultural and natural monuments, as well as for forests in general and landscape characterizing or shaping areas, respectively for landscape conservation and protection, there are distance regulations of 500 to 1000 meters, but in most cases, this is decided on a case-by-case basis.

Medicinal springs and drinking water areas are protected areas, so it is forbidden to build wind turbines there. Around standing waters and water protection areas, a distance of 50 up to 1000 meters is to be kept. For banks and dikes on water bodies and sea coasts, as well as floodplains and flood protection areas and wetlands according to *Ramsar*<sup>5</sup> conventions, this applies for 10 up to 1000 meters.

Furthermore, in some places height restrictions have to be considered, for example of 100 meters. In addition, there are sometimes minimum area sizes of 20 to 35 hectares or 3 wind turbines and spacing requirements of suitability areas of wind use of 2500 to 5000 meters. Finally, in some federal states, it must be noted that certain wind conditions must be given: Often depending on the individual case, an average wind speed of 5.3 to 5.75 meters per second must be reached at a certain height above the ground.

## 2.2. Algorithm

Based on the previously described distance regulations, a map is now to be created in which it is marked where wind turbines of certain types can be planned.

The starting point of this work is geographical data of objects in the considered area taken from GIS files. *GIS* is the abbreviation for the geographic information system. The GIS data format is provided by geographic information systems. In the present work, data provided by OpenStreetMap<sup>6</sup> is used. Compliance with the spacing rules is ensured as follows: After loading the region data, the area to be built on is divided into squares so that the wind turbines will be planned on a square grid. The size of squares can be chosen freely and adjusted accordingly in the code. A reasonable size would be for example squares of 20×20 square meters because this could roughly correspond to the area of a house.

Then, squares that contain an object for which there are distance regulations, like highways, buildings, or airports, are identified. Every square that contains at least a part of these objects is marked as an object square. For example, if a square contains a part of an airport area, it will have the property *airport* from now on.

---

<sup>4</sup>Habitats Directive for Germany (FFH) <http://www.fauna-flora-habitatrichtlinie.de/>. Accessed 24 Apr 2022.

<sup>5</sup>Website Ramsar <https://www.ramsar.org/>. Accessed 24 Apr 2022.

<sup>6</sup>Create GIS files based on OpenStreetMap [https://wiki.openstreetmap.org/wiki/GIS\\_software](https://wiki.openstreetmap.org/wiki/GIS_software). Accessed 24 Apr 2022.

In order to identify neighboring squares that must not be built on due to distance rules, the nearest neighbor within the set of already marked squares for each previously unmarked square is searched for:

Therefore a  $k$ -d-tree is constructed. A  $k$ -d tree is a search tree with  $k$  dimensions. In the root and the inner leaves, coordinates of the borders between some squares are stored, while in the leaves the coordinates of individual squares are stored. The higher the hierarchy level, on which the coordinates for separating several squares are stored, the more squares are separated by them: in the root, the coarsest division into smaller components is made, which is refined more and more towards the leaves.

The coordinates of object squares are stored in the leaves of the  $k$ -d-tree. By partitioning all squares by the root and inner nodes as described, the nearest object square can thus be found for each previously unmarked, i.e. free, square. This is possible with a single pass because at each inner node the child is chosen in whose region the considered free square lies.

The use of a  $k$ -d tree makes sense because the search for the nearest objects is considerably faster than a brute-force search. Otherwise, for each square, every single cell in the environment would have to be examined for its property, whereas in the search tree only this one pass is required.

In Herzogenrath, for example, the area is divided into  $n = 521$  squares. For a brute-force search,  $n$  squares would require

$$n \cdot (n - 1) \tag{1}$$

steps, because for each square every other one would have to be examined. For  $k$ -d-trees, on the other hand, a runtime of

$$O(n \cdot k + \log_2(n)) \tag{2}$$

is expected for its construction, but the search requires only

$$O(n \cdot \log_2(n)) \tag{3}$$

steps. So for the brute-force search  $521 \cdot 520 = 270920$  steps are needed. Computing the  $k$ -d tree takes  $521 \cdot 3 + \log_2(521) \approx 1572.03$  steps, and then searching all 521 squares takes  $521 \cdot \log_2(521) \approx 4702.10$  steps. So here there is an improvement of at least  $270920 - (1573 + 4703) = 264644$  steps by using the  $k$ -d tree. Therefore, the runtime can be reduced by about 98%.

The resulting map is called "base map". In the implementation, the calculation of the base map with the use of the  $k$ -d-tree takes less than five seconds and for each wind turbine type then only fractions of a second.

Now it can be searched for the nearest object of a type for each still unmarked cell and check whether the required minimum distances are kept. Initially, this is done only for those objects whose distance is independent of the turbine type, i.e., independent of rotor diameter and height of neighboring turbines. By doing so, a base map is created. The squares are then examined for their proximity to objects to which the distances

may vary depending on the turbine type and scenario setting. In particular, distances to houses are considered. Details on chosen turbine types can be found in Appendix 9 and for the resulting specific observations see Section 5.1.

It is possible to have the area that can be used for planning wind turbines (potential area for short) calculated for different distances to houses. A user of the software can make specifications in meters, otherwise, the calculation is made with the recommendation or specification about that distance of the respective federal state, which is usually known by the software. Otherwise, there is a default value of a distance of 500 meters.

It has to be considered that too large distances can lead to the fact that the planning of wind turbines in the considered area is no longer possible. In the region of the case study Herzogenrath, this happens when the minimum distance to houses of 1000 meters recommended by North Rhine-Westphalia is used.

In summary, this means that squares are searched which are too close to the objects under consideration, according to the regulations - all unaffected squares are designated as potential areas. The flowchart can be taken from Figure 2, and Figure 3 exemplifies this procedure.

---

<sup>7</sup>Erlass für die Planung und Genehmigung von Windenergieanlagen und Hinweise für die Zielsetzung und Anwendung (Windenergie-Erlass) [https://recht.nrw.de/lmi/owa/br\\_bes\\_text?anw\\_nr=1&gld\\_nr=2&ugl\\_nr=2310&bes\\_id=38805&val=38805&ver=7&sg=0&aufgehoben=N&menu=1](https://recht.nrw.de/lmi/owa/br_bes_text?anw_nr=1&gld_nr=2&ugl_nr=2310&bes_id=38805&val=38805&ver=7&sg=0&aufgehoben=N&menu=1). Accessed 24 Apr 2022.

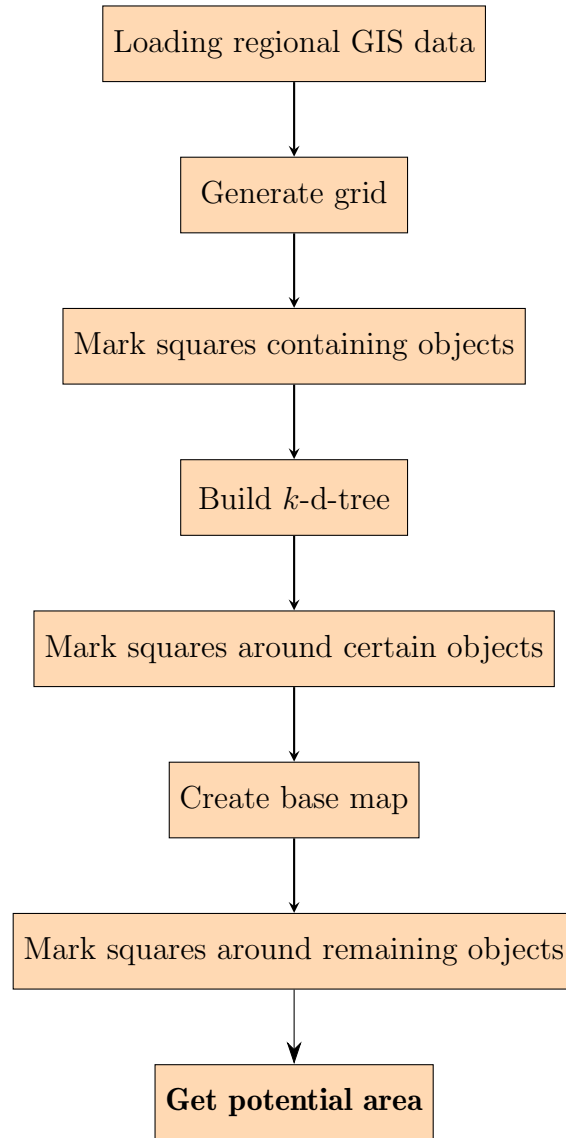


Figure 2: Flowchart of the algorithm to determine the potential area.

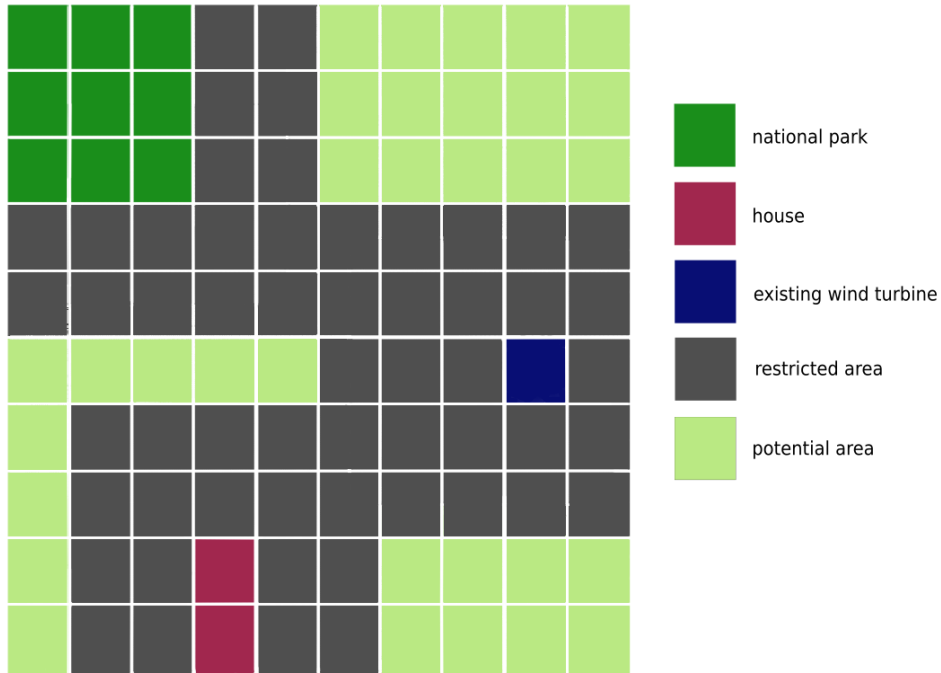


Figure 3: Example for the determination of the potential area for wind turbine planning. Each square represents an area of  $200 \times 200$  square meters. The dark green squares are meant to represent the edge of a national park, the red squares represent a house, and the blue square symbolizes an already standing wind turbine. Based on the restrictions of the state of North Rhine-Westphalia, a recommended minimum distance of 300 meters has to be kept to the national park<sup>7</sup>. Furthermore, it is assumed that the wind blows mainly in a straight line from west to east (so from left to right in the figure) and that the wind turbine has a rotor diameter of 100 meters. It is decided that there should be no other turbine within 500 meters in the main wind direction and within 300 meters horizontally to reduce the wake. The house stands alone and it is assumed that in an individual case decision it was decided that a distance of at least 400 meters should be granted. The dark grey areas now represent the areas where in no case a wind turbine should be planned. All remaining, not yet marked squares are now marked as potential areas, here in light green.

### 3. Energy Yield Forecast

In order to generate as much energy as possible with a wind farm, it is necessary to find an optimum of the highest possible number of energy-generating wind turbines and the greatest possible freedom from interference because of the wake effect in the conversion of wind energy into electrical energy.

A reasonable approach to measure the efficiency of a wind farm layout is to optimize the values of annual energy production (AEP) and levelized cost of energy (LCOE), for example, shown by Lo [59].

The AEP is the value for the electrical energy produced in a year. The LCOE is the minimum cost for which the electrical energy must be sold to make neither a loss nor a profit on that sale. Since profit is desired, the LCOE should ideally be as low as possible, while the AEP should be maximized.

#### 3.1. Regional Wind Data

To be able to give an expectation of the energy generated annually, the turbine type, wind direction, and wind speed must be considered. The wind speed at the rotor of a turbine is of particular importance, since, as already explained, neighboring turbines can influence it.

For this calculation, all turbines up to a certain distance around the considered region should also be included. This is because their wake effects can have an influence on the energy production of the newly planned wind turbines. Thereby 2000 meters is a reasonable distance because this often corresponds to about 20 times the rotor diameter  $D$ . At this distance or greater, the wake effect should hardly matter.

In addition, the wind speed values must be included. The measurement height  $h_{\text{measured}}$  is here, as usual for weather stations, at 10 meters. The used data is obtained from the German Weather Service<sup>8</sup>. From the given wind speeds  $u_{\text{measured}}$ , one can estimate the wind speed of the turbines  $u_{\text{turbine}}$  at hub height  $h_{\text{hub}}$ .

Therefore, a simplified formula is used, where the Kleeman-Meliß exponent is used, which depends on whether and how densely objects are distributed on terrain as mentioned by Kleeman and Meliß [35]:

$$u_{\text{turbine}} = u_{\text{measured}} \cdot \left( \frac{h_{\text{hub}}}{h_{\text{measured}}} \right)^g. \quad (4)$$

The Kleeman-Meliß exponent  $g$  is assigned as shown in Table 1.

From the transferred data of the preceding calculations, a matrix is calculated, whose rows stand for the calculated wind speeds and whose columns stand for the wind directions.

---

<sup>8</sup>Wind data for wind energy users [https://www.dwd.de/DE/leistungen/winddaten\\_windenergienutzer/winddaten\\_windenergienutzer.html](https://www.dwd.de/DE/leistungen/winddaten_windenergienutzer/winddaten_windenergienutzer.html). Accessed 24 Apr 2022.

	$g$
Open terrain (water, grassland, farmland, coastline, deserts etc.)	0.16
Terrain with obstacles up to 15 meters (forests, settlements, cities etc.)	0.28
Terrain with big obstacles (big cities etc.)	0.40

Table 1: The Kleeman-Meliß exponent depending on the terrain, see Kleeman and Meliß [35]. In brackets additionally examples of the respective descriptions, according to which the exponent is to be chosen.

The values of the wind speed must be between a defined minimum and maximum speed each. No power is generated at the turbines below or above these values. The reason for these speed limits is that if the wind speed is too low or too high, the wind energy cannot be converted into electrical energy. At too low wind speeds, this is due to friction, and at too high speeds it is due to the need to protect the turbine from damage caused by too fast rotation.

The minimum wind speed is called cut-in speed and the maximum cut-out speed. These depend on the turbine type and are specified by the manufacturer.

Accordingly, the entries of the aforementioned matrix are then information about expected hours per year with the respective wind speed and direction.

Based on this, a wind rose can be designed. This is a plot of wind speeds for different wind directions. All possible wind directions are divided into discrete steps for the wind rose. The step size can be adjusted depending on the available information. Common wind roses are often divided into 10° to 45° steps.

For the app, a step number of 30 degrees is chosen and it is worked with files in EnergyPlus Weather (EPW) format. These contain weather data such as wind conditions for the last years<sup>9</sup>.

Figure 4 shows the distribution of wind directions in Herzogenrath. In addition, Figure 5 provides information on the distribution of wind speeds for the respective wind direction range. The considered range of speeds is chosen according to cut-in and cut-out speeds of the selected turbine types for my case study, see Section 5. There, the data presented here is evaluated and consequences resulting from it are explained. The corresponding specific cut-in and cut-out speeds can be taken from Appendix 9.

For simplification, a "main wind direction" is determined. To do this, the wind data over several years in the respective region are looked at and the wind direction from which the wind blows most frequently is selected. For this purpose, the frequencies of the wind directions for angles differing by 180° are summed up.

This procedure can be used to simplify the following calculations because it is internally the same for wind farms whether the wind blows "from the front" or "from the back", i.e., 180° different. The result is shown graphically in Figure 6.

<sup>9</sup>EnergyPlus Weather File (EPW) Data Dictionary <https://bigladdersoftware.com/epx/docs/9-3/auxiliary-programs/energyplus-weather-file-epw-data-dictionary.html>. Accessed 24 Apr 2022.

Weather data for Germany [https://climate.onebuilding.org/WMO\\_Region\\_6\\_Europe/DEU\\_Germany/index.html](https://climate.onebuilding.org/WMO_Region_6_Europe/DEU_Germany/index.html). Accessed 24 Apr 2022.

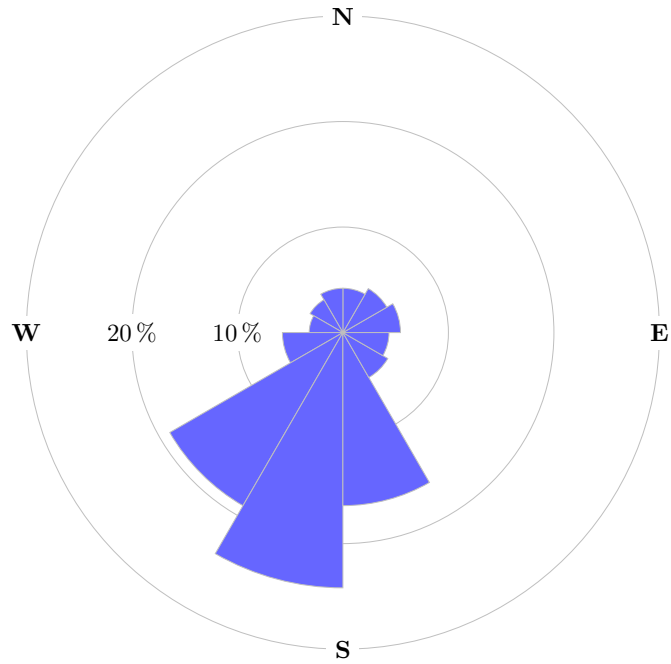


Figure 4: Distribution of wind directions for Herzogenrath in steps of 30°.

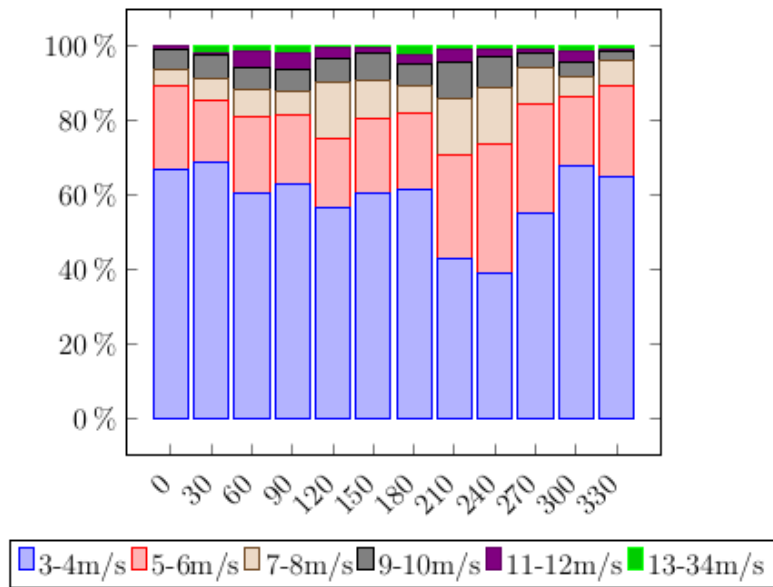


Figure 5: Distribution of wind speeds for Herzogenrath corresponding to cut-in and cut-out speeds of my selected turbine types, see Table 9.

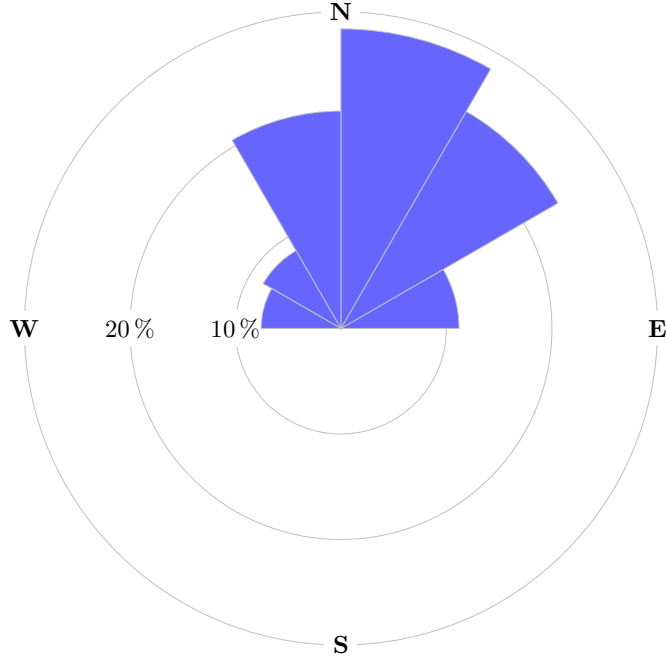


Figure 6: Distribution of the summarized opposite wind directions for Herzogenrath in steps of  $30^\circ$ .

To simplify the calculation, then the coordinates are adjusted so that the wind always comes from the main wind direction, and the whole situation is simulated depending on the given wind speed according to the PARK model, see Section 3.3.

### 3.2. Annual Energy Production

Based on the turbine information and the wind conditions, finally, the generated energy can be calculated, as presented by Lo [59]:

$$E_{\text{AEP}_{\text{gross}}} = (8760h + 6h) \cdot \sum_{i=1}^{N_{\text{dir}}} \left( \sum_{u=u_{\text{cut-in}}}^{u_{\text{cut-out}}} w(\varphi_i, u) \cdot P_{\text{farm}}(\varphi_i, u) \right) \quad (5)$$

The number of hours results from the average number of hours in a year: the additional six hours come from the equal division of leap years. The parameter  $N_{\text{dir}}$  stands for the number of considered wind directions. The larger the number, the more accurate the result, but the more complex the calculation. The function  $w(\varphi_i)$  describes the probability for the wind direction  $\varphi_i$ . The limits of the second sum  $u_{\text{cut-in}}$  and  $u_{\text{cut-out}}$  are the already mentioned fixed velocities between which results are evaluated.  $P_{\text{farm}}(\varphi_i, u)$  gives the value for the generated power of the wind farm under given wind direction  $\varphi_i$  and wind speed  $u$ .

The generated power of the wind farm  $P_{\text{farm}}(\varphi_i, u)$  is calculated with

$$P_{\text{farm}}(\varphi, u) = \sum_{k=1}^{N_{\text{turbines}}} P_k(u_0(k, \varphi)) \quad (6)$$

where  $\varphi$  is still the wind direction and  $u$  the wind speed.  $N_{\text{turbines}}$  is the number of wind turbines considered,  $P_k$  stands for the generated power of turbine  $k$ , and  $u_0(k, \varphi)$  is the wake speed of turbine  $k$  depending on wind direction and speed. I describe its calculation in Section 3.3.

So in the upper formula for the gross EAP, for all discretized wind directions (see Section 3.1), weighted by their probability, the generated energy of the wind farm for one year is summed up.

Thus, for all wind direction steps the generated energy is calculated, taking into account their probabilities and wind speeds, as well as from the wind loss described above.

After this calculation in the code, the AEP for each turbine is output and stored. This gives a meaningful indicator of the overall productivity of newly planned turbines and existing turbines affected by new ones. Energy loss caused by turbulence from newly planned turbines can be estimated.

### 3.3. PARK Turbulence Model

To calculate the disturbance of turbines close to each other, the PARK wake model is used. This frequently used model is relatively simple to implement and gives a good basis for estimating energy losses. In it, the assumption is made that the propagation of the wake is linear and spreads in wind direction conically starting from the turbine. This propagation depends on the hub size and surface roughness of the rotors as explained at Lo [59]. It thus becomes wider starting from the area behind the rotors of the considered turbine, coming from the wind direction.

With the same weather conditions on the whole area of a wind farm, there can still be different values for individual wind turbines, even of the same design. This is because the wake is also affected whether one turbine is affected by the wake of another (whether it is downstream of at least one other turbine).

For a turbine  $k$  the initial wind speed in front of the turbine  $u_0(k)$ , the velocity-dependent thrust coefficient of the turbine  $C_t(u_0(k))$ , which is given by the wind turbine manufacturer, the rotor diameter  $D_k$ , the wake decay  $k_w$ , and the wake loss  $\ell_{\text{wake}}$  are considered.

According to Lo [59], the wind speed  $u_w(x)$  at a point  $x$  behind the turbine  $k$  can then be calculated using the following formula:

$$u_w(x) = \beta_k \cdot \left( u_0(k) - \frac{1 - \sqrt{1 - C_t(u_0(k))}}{(1 + \frac{2k_w \cdot x}{D_k})^2} \cdot \ell_{\text{wake}} \cdot u_0(k) \right) \quad (7)$$

The wake decay  $k_w$  is calculated with

$$k_w = \frac{0.5}{\log_{10}(\frac{h_{\text{hub}}}{z_0})} \quad (8)$$

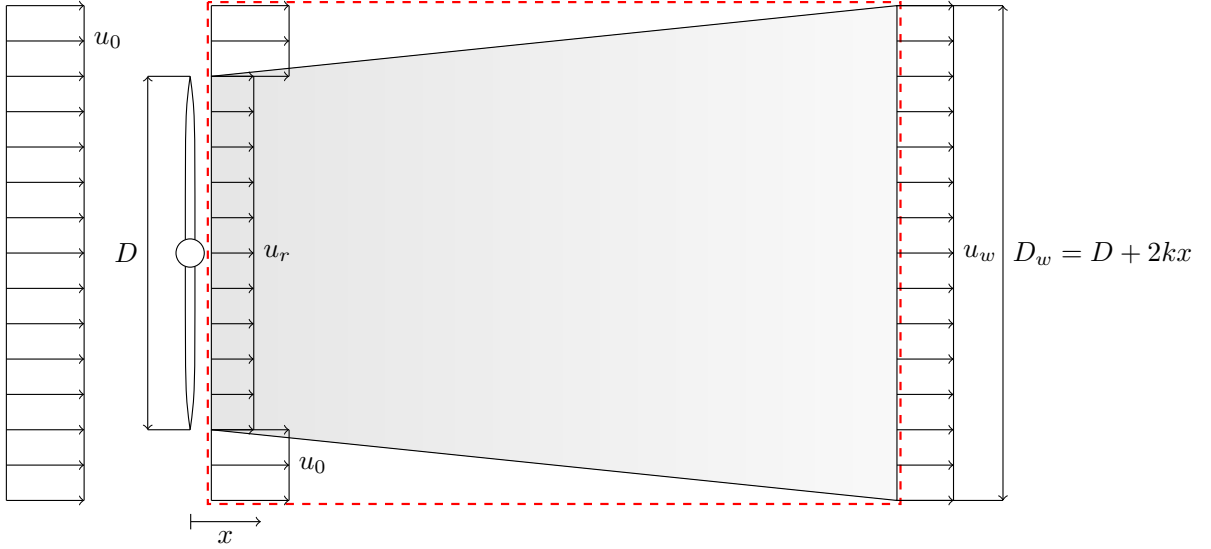


Figure 7: Propagation of the wake according to the PARK model. The velocities  $u_0$  and  $u_r$  represent those in the undisturbed free wind flow and directly behind the turbine rotors [28].

where  $h_{\text{hub}}$  is again the hub height and  $z_0$  is the surface roughness.

The wake radius thus grows with a factor  $k_w$ . Graphically this can be represented by adding the wake diameter  $D_w = D_w(x)$ , i.e. the diameter of the plane area affected by the wake effect. This grows linearly by  $2 \cdot k_w$ , see figure 7 from Heiming [28].

As an approximation for the surface roughness, the values from table 2 can be used.

If the turbine under consideration is completely covered by the wake of another turbine,  $\beta_k$  is set to 1. This is the shadowing factor. It is calculated if a turbine is partially shaded by the wake of another turbine  $j$ , as follows:

$$\beta_k = \frac{A_{j,\text{wake}}}{A_k}. \quad (9)$$

$A_k$  is the value for the circular area of turbine  $k$  and  $A_{j,\text{wake}}$  stands for the intersection area of the rotor from turbine  $k$  with the wake from turbine  $j$ , which is visualized in Figure 8.

### 3.4. Levelized Cost of Energy

Before the determination of the value of the LCOE can be done, some other costs must be known or calculated.

Elkinton [18] proposes a formula that includes the parameter of investment cost  $C_{\text{invest}}$ .

<sup>10</sup>Typical values for  $z_0$  <https://www.wind-energy-the-facts.org/fundamentals.html>. Accessed 24 Apr 2022.

Type of terrain	$z_0$ in meters
Mud Flats, ice	0.00001
Sand	0.0003
Snow surface	0.001
Bare soil	0.005
Low grass, steppe	0.01
Fallow field	0.03
Open farmland	0.05
Shelter belts	0.3
Forestand woodland	0.5
Suburb	0.8
City	1

Table 2: Common values for the surface roughness of onshore wind farms<sup>10</sup>, depending on the soil.

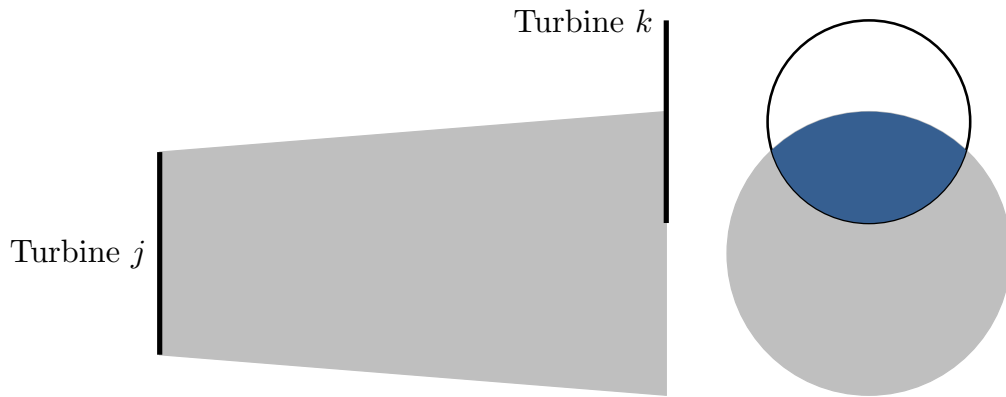


Figure 8: On the left side two locally offset turbines with only partial influence of the wake effect from a top view. The straight lines represent the rotor diameters and the gray area the wake coming from there. On the right, in blue the intersection of the wake cross section with the circular area of the turbine affected by the wake [28].

Here, costs for project management  $C_{\text{project}}$ , logistics (here the cost of the substation  $C_{\text{substation}}$  because there is generally only one of these onshore, unlike for offshore wind farms), labor costs for laying the cables and cable material cost  $C_{\text{cabling}}$ , turbines  $C_{\text{turbine}}$ , and individual turbine foundations  $C_{\text{foundation}}$  are summarized. Expressed as a complete formula, this would be:

$$C_{\text{invest}} = C_{\text{project}} + C_{\text{substation}} + C_{\text{cabling}} + \sum_{k=1}^{N_{\text{turbines}}} \left( C_{\text{turbine}}(k) + C_{\text{foundation}}(k) \right). \quad (10)$$

In addition, the annual operation and maintenance cost is included. This is calculated as follows:

$$C_{\text{O\&M}} = C_{\text{MWoperation}} \cdot \sum_{k=1}^{N_{\text{turbines}}} P_{\text{max}}(k). \quad (11)$$

$C_{\text{MWoperation}}$  is the cost for operation of 1 MW.

Now an equation for the levelized cost of energy is developed by adding discount/interest rate  $r_{\text{rate}}$  and expected lifetime of the wind farm in years  $N_{\text{lifetime}}$ , following Elkinton's [18] formula:

$$\pi_{\text{LCOE}} = \frac{C_{\text{invest}} \cdot \frac{(1+r_{\text{rate}})^{N_{\text{lifetime}}} \cdot r_{\text{rate}}}{(1+r_{\text{rate}})^{N_{\text{lifetime}}}-1} + C_{\text{O\&M}}}{E_{\text{AEP}}}. \quad (12)$$

This should now be the objective function for my optimization since costs can be minimized and energy output maximized at the same time. In the following, I will compare unit cost per unit power output. That value should be minimal.

## 4. Optimal Positioning

Now the goal is to place wind turbines as economically advantageous as possible on the considered area, in compliance with recommendations and regulations, according to the potential area, see Section 2.

For this purpose, I will present two approaches: An optimization with wind turbines of a certain type, i.e. of the same height, and an approach for planning wind turbines of different heights within one area.

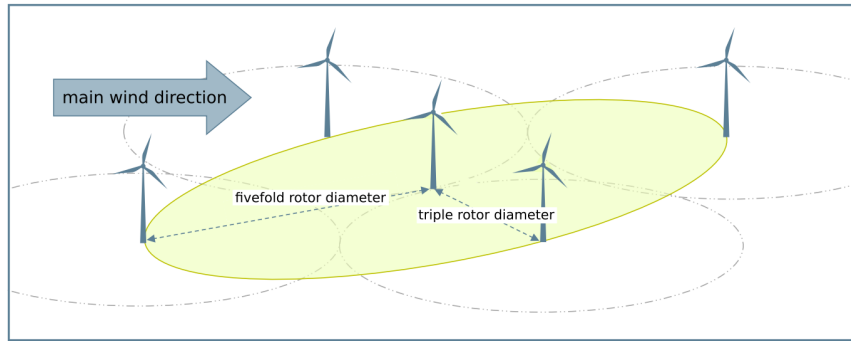


Figure 9: Illustration of the  $3D/5D$  rule. The gray arrow marks the main wind direction and the ellipses around turbines<sup>12</sup> were constructed by spacing  $5D$  in the main wind direction and  $3D$  orthogonal to it.

## 4.1. Optimal Positioning of Wind Turbines with One Clearly Defined Hub Height

In addition to the rules on what distances wind turbines should have at least to certain surrounding objects, their distances to each other must also be considered. The *Fachagentur Windenergie an Land*<sup>11</sup> recommends a distance of at least five times the rotor diameter in the main wind direction and orthogonally at least a distance corresponding to three times the rotor diameter to avoid the wake effect. I already mentioned this before as the  $3D/5D$  rule.

It is illustrated by Figure 9 and an algorithm based on this is further described in the following section.

### 4.1.1. Ellipse-Based Algorithm

The basis of the algorithm are the region maps, which were created after the execution of the algorithm for the potential area, see Section 2.2.

So, in this, for the respective squares into which the region has been divided, the object type is stored or the marker "potential area" is added.

To calculate a specific arrangement of wind turbines in the desired region, now each of these region maps is processed in the order in which they were created. For this purpose, a file with the data from the calculation of the potential area is passed to the calculation of the optimization. This file also contains information about the turbine types to be used, whose rotor diameter is important in the following.

The procedure can be taken from Algorithm 1:

It is started per scenario that a direction is chosen in which, starting from points at

<sup>11</sup>Overview onshore wind energy, 2019 [https://www.fachagentur-windenergie.de/fileadmin/files/Veroeffentlichungen/Faktenpapiere/FA\\_Wind\\_Hoehenbegrenzungen\\_Wind-an-Land\\_03-2019.pdf](https://www.fachagentur-windenergie.de/fileadmin/files/Veroeffentlichungen/Faktenpapiere/FA_Wind_Hoehenbegrenzungen_Wind-an-Land_03-2019.pdf). Accessed 24 Apr 2022.

<sup>12</sup>Overview onshore wind energy, 2019 [https://www.fachagentur-windenergie.de/fileadmin/files/Veroeffentlichungen/Faktenpapiere/FA\\_Wind\\_Hoehenbegrenzungen\\_Wind-an-Land\\_03-2019.pdf](https://www.fachagentur-windenergie.de/fileadmin/files/Veroeffentlichungen/Faktenpapiere/FA_Wind_Hoehenbegrenzungen_Wind-an-Land_03-2019.pdf). Accessed 24 Apr 2022.

the edge of the region, wind turbine locations are searched for. This direction is called the "alignment direction".

The starting point is always at one corner of the square area and the line is moved

---

**Algorithm 1** Ellipse-based algorithm in pseudo code

---

- 1: Loading potential area data and turbine information
  - 2: Choose alignment direction and step size
  - 3: According to the alignment direction set two sides of the selected rectangular region as the boundary for the following observations
  - 4: Take the points on the other two sides as entry points for the line in alignment direction from line 2, which will be moved across the surface starting from these points
  - 5: **while** Alignment directions not yet investigated available **do**
  - 6:     **while** Entry points not yet investigated available **do**
  - 7:         Go to the next entry point (at the very beginning go to the first entry point)
  - 8:         Starting from this point, check each square step by step in the selected direction until reaching one of the boundaries defined in line 3 to see if it belongs to the potential area
  - 9:         **if** Potential area square found in alignment direction **then**
  - 10:             Place wind turbine on this square
  - 11:             Remove area around wind turbine from potential area according to the main wind direction and  $3D/5D$  rule
  - 12:         **else**
  - 13:             Break (Change alignment direction according to selected step size)
  - 14: Compare the results for the alignment directions
  - 15: Store and output optimal placement
- 

square by square along the border of the region to the diagonally opposite corner. The starting point depends on the alignment direction, more precisely its angle and orientation.

The angle and orientation of the alignment direction are important because the line is created in such a way that it has two intersections with the surface boundary of the region under consideration. Because of the square shaped area only one corner is possible. The two adjacent sides are those for the entry points in the following. The other two limit the line in alignment direction, more about this below.

However, the chosen alignment direction can also have a decisive influence on the number of suitable wind turbines, therefore the whole procedure is performed for different angles.

The calculations are done for all possible directions with a number of starting points that can be freely set. This defines the step size. So for a number of  $n$  starting points steps at intervals with a difference  $s$  of

$$s = \frac{2 \cdot 180^\circ}{n} \tag{13}$$

are considered: starting at  $0^\circ$  up to  $180^\circ - s$  in and against the main wind direction, see Section 3.1.

As soon as the line intersects a potential area, a wind turbine is planned at this location and the area of an ellipse around the turbine is no longer considered a potential area. This means that the marking of the corresponding squares can no longer be "potential area". The affected squares of the eliminated ellipse-shaped area are determined according to the main wind direction and the  $3D/5D$  rule presented in Section 4.1, see also Figure 9.

So, after a turbine location is planned, it is investigated to the border of the region along the line whether other possible turbine locations can be located, otherwise, the line is moved in the given direction, i.e. to the next point at the edge of the area.

This procedure is carried out until the area has been examined in all alignment directions. Since these searches always cover two edges of the area according to the alignment direction, this ensures that there is no potential area left after the process is finished. This will result in the maximum number of turbines for the appropriate settings.

In Appendix B.1 the algorithm can be understood by means of plots which show step by step an exemplary turbine positioning. Here it is illustrated how new turbine positions are systematically found by shifting a straight line:

In Figures 10 to 21 always two possible turbine locations are found on a straight line shifted in between. From Figure 21 to Figure 22 it can then be observed how a turbine is planned at a greater distance, which is due to the potential area for the given conditions. The corresponding potential area is illustrated in Figure 29. Accordingly, one can see from the final turbine distribution in Figure 26 that the potential area was fully filled with wind turbines, according to the algorithm described here.

From the results of these calculations, the one that can accommodate the maximum number of turbines in the region is chosen. If several solutions come up with the same number, the angles of the horizontal to the main wind direction and the chosen alignment direction are compared. Then the solution whose angle is the smallest for this is picked.

#### 4.1.2. Refinement Step

As described in the previous section, the maximum number of wind turbines that can be reasonably built in the given region is found. However, their placement can be optimized even more finely by reconsidering the already determined turbine positions locally in each case.

The starting point for the refinement is thus a given area with several turbines planned on it, as well as their associated potential areas from Section 4.1.1.

The local optimization of the placements assigned to the wind turbines is based on increasing the distances between each turbine while keeping the general number of turbines constant. To do this, a factor  $\xi$  is added to the ellipse parameters and increased incrementally: So it should no longer be three or five times the rotor diameter, but

maximizing these values. Therefore they are multiplied each by the gradually changed coefficient  $\xi$  and checked whether the same number of turbines can still be placed on the area under consideration of the new distance between the turbines. The specific procedure can be found in Algorithm 2. If the same number of turbines as before can still be placed, the factors are tried to increase further. Otherwise, a smaller value is subtracted and the test is repeated. The exact procedure can be taken from Algorithm 2.

Since  $\xi$  must logically be less than 1, because otherwise more turbines could be planned with the original  $3D/5D$  rule, the initial value for changing  $xi$  is 0.16: this is then the middle of the possible values between 0 and 1 that could possibly occur with the binary procedure described.

Thus,  $\xi$  is now maximized with the constraint that the number of turbines remains.

---

**Algorithm 2** Refinement step for ellipse-based algorithm in pseudo code

---

- 1: Start with turbine positioning for distances with three and five times rotor diameter: Save maximum number of turbines
  - 2: Set coefficient difference  $\delta = 0.16$  and coefficient  $\xi = 1$
  - 3: Increase distance by 1.16 ( $= \delta + \xi$ ) and calculate turbine positioning
  - 4: **while** Maximum number of turbines not reached or difference  $\delta > 0.01$  **do**
  - 5:     **if**  $\delta > 0.01$  **then**
  - 6:          $\xi := \xi + \delta$
  - 7:     **if** Maximum number of turbines not reached **then**
  - 8:         **if**  $\delta > 0.01$  **then**
  - 9:              $\delta := \delta/2$
  - 10:          $\xi := \xi - \delta$
  - 11: Store maximum  $\xi$  and associated turbine positioning
- 

When the maximum value is found with a chosen accuracy, the output is stored.

In the specific implementation, an accuracy value of 0.01 is used. This means that  $\xi$  is maximized to the hundredths place.

So the distances between the individual wind turbines are maximized for the given number of them. This means that the wake effect plays a smaller role and therefore the AEP increases. In this way, the costs remain nearly the same (for example, cable costs are rising, but this is not a significant factor onshore), but the generated energy can be increased.

Therefore the LCOE decreases and this corresponds to the goal of minimizing the cost per unit power.

## 4.2. Optimal Positioning of Wind Turbines with Different Hub Heights

The ellipse-based approach works in the present version only for the planning of wind turbines of one certain type for a region. So, in case there are different wind turbine

types to choose from, an optimal placement can be found for each one. An approach that considers a mix of some given wind turbines in a region as an additional possibility is described below.

Another difference from the ellipse-based algorithm is that there a target function is used to plan a maximum number of turbines until a fixed limit (for the result of the function) is reached.

#### 4.2.1. Greedy Algorithm

Previously published literature (among others: K. Chen et al. [8, 9], Y. Chen et al. [11], Chowdhury et al. [12, 13]) suggests that the use of a mixture of different turbine types in a region can further minimize wake effects, which would result in the desired impact on minimizing cost per unit power.

I implemented the algorithm of Chen et al. [9], which is relatively simple but very efficient. The procedure can be found as pseudo code in Algorithm 3 and is as follows:

First, the area under consideration is divided into two-dimensional squares again, i.e.

---

#### **Algorithm 3** Greedy algorithm in pseudo code

---

- 1: Loading potential area data, already existing turbines in the neighborhood, and turbine information
  - 2: Set a maximum LCOE that should not be exceeded in the following
  - 3: **while** Turbine types not yet investigated available **do**
  - 4:     Choose the next available turbine type from the list of types
  - 5:     **if** Free squares available in the potential area of the considered turbine type **then**
  - 6:         Calculate the LCOE for each square of the potential area according to the turbine type, also taking into account the possible wakes from or for other neighboring turbines
  - 7:         Compare the results and select the square with the lowest result and save its coordinates and LCOE
  - 8:     **else**
  - 9:         Delete the turbine type from the list of available turbine types
  - 10: Compare values of the best squares for all of the turbine types and choose the lowest one
  - 11: **if** Best LCOE not greater than chosen maximum LCOE **then**
  - 12:     Place a turbine of the corresponding type on this square
  - 13: **else**
  - 14:     Discard the results from this step and break
  - 15: Store and output optimal placement
- 

a grid is projected onto it. The coordinates can be the same as for the determination of the potential areas. The individual squares are then again numbered consecutively. In the following, the squares are evaluated according to an objective function whose result at the end should be optimal for the whole terrain. Chen et al. there propose

minimizing an objective function like the calculation of the LCOE, see Section 3.4.

The chosen function is now calculated per step on each free square of the potential area of each available wind turbine. Then, the respective best possible values of all turbine types are compared and a turbine of the type with the best result is placed on the corresponding square. The possible wake effects of existing turbines in the region are also included and then, of course, that of the newly planned turbines.

The calculation is only applied inside the already determined potential area. If more than one position is possible, the one with the lowest number is chosen, according to the numbering of the squares made at the beginning.

Chen et. al. [9] specify a target number of turbines in their algorithm, for which the algorithm terminates when it is reached.

At this point, I deviate in my approach: Instead, a user has to set a maximum LCOE value in advance that must not be exceeded and carry out wind turbine planning until this value would be exceeded. In this way, it is tried to place as many wind turbines as possible in the area, within the limits of costs per generated energy that a user considers acceptable.

#### 4.2.2. Refinement Step

Furthermore, the aforementioned paper by Chen et al. [9] refers to an adjusting step developed by Chen et al. [6].

In the order in which the newly planned turbines were added, they are now considered individually again. So it is started with the first one which is removed from the planning. Then the objective function value is calculated again for each free square of the region and the turbine is inserted on the square with the best result. This is repeated for each of the turbines.

When all the turbines have been re-examined in this way, a comparison is made to see if the resulting layout is the same as the original. If it is not, the described procedure is repeated for the turbines with the new layout. Otherwise, the refinement step is completed and the newly created layout is the result.

But according to the Chen et al., it doesn't change the result much, and omitting it of course saves calculation costs, so this will not be considered further here.

## 5. Case Study

To illustrate the previous considerations, I will now calculate and classify the results using the region of Herzogenrath near Aachen as an example.

Here, an area of about 35 000 kilometers is considered and a square size of  $20 \times 20$  square meters is chosen for the grid.

The procedure now is that first the GIS data is read from OpenStreetMap. Then there is a search for objects for which there are distance regulations in the region and mark them accordingly.

The resulting map is used to determine the area that can be used for wind turbine planning in the following, i.e. the potential area. Here, several maps are created: As already described in Section 2, on the one hand the possibility to keep different distances to houses should be given. Because also different distances to certain objects depending on the type of the wind turbines have to be kept, a case distinction has to be made here as well. So there are house distance times turbine type number many cases per scenario. This is discussed in more detail in Section 5.1.

Before the wind turbine positioning can finally be planned, the calculation of regional wind data on the considered area is performed, compare Section 3.1.

In any case, wind turbine planning is done using the ellipse-based algorithm, compare Section 4.1.1. This is done either for all cases obtained from the determination of the potential area or only for selected ones. This can be worthwhile, for example, if there were a lot of cases or some were more promising, such as having larger areas as a result. Also, a choice can be made whether to optimize with the greedy algorithm, see Section 4.2.1. If this is the case for the corresponding scenario, then the wind turbine planning is also done with that.

## 5.1. Potential Area

In the example region Herzogenrath, distances to buildings, highways and motorways, water protection areas, and furthermore already existing wind turbines are considered. Now, areas for different distances to houses and different turbine types should be compared. The distances and types are arbitrarily chosen so that the deviations are relatively large in each case and thus can be compared well. The turbine types are selected from types already standing in and around Herzogenrath and Soest, as these locations are the test regions of the underlying app under development.

Since the positioning depends on the respective hub height  $H$  and rotor diameter  $D$ , an overview of these properties of the used turbine types is given in Appendix 9. Moreover, there is the additionally arbitrarily defined "Test Turbine" in order to be able to show already differences in the size of the potential area between the different turbine types. As you can see in Table 3, the results for all real existing turbine types for Herzogenrath are the same. Obviously, the position of the regional objects is such that the potential area is only changed when the rotor diameter of a turbine is very large. The only objects with distance regulations depending on the rotor diameter of the newly planned wind turbines are other surrounding already standing turbines.

However, the house distances of the examples will be increased significantly for the consideration of the optimization results, because the area should be more constrained there. This is explained in the evaluation of the results, see Section 5.2.

Plots for the potential areas of all example scenarios can be found in Appendix B.2. It can be clearly seen how the potential areas become smaller the greater the distance to houses is selected. The scales of the plots are adjusted accordingly, so that the distribution of the area can be followed well in each case. The potential area for Herzogenrath according to the corresponding conditions is always shown completely.

<b>Turbine type/Minimal house distance</b>	100 meters	200 meters	500 meters
W5200/750	59536 squares	14970 squares	670 squares
MM82	59536 squares	14970 squares	670 squares
Test Turbine	58816 squares	14759 squares	670 squares

Table 3: Size of the potential area for different turbine types in combination with different minimum distances to surrounding houses.

## 5.2. Optimal Positioning and Energy Yield Forecast

Based on the collected data from Section 3.1, see also the wind rose in Figure 6, the wind in Herzogenrath blows most often at the angle of  $60^\circ$ . This is what is called the "main wind direction". For the main speed, the frequency of occurring wind speeds from 3 to 34 meters per second is considered, taking into account the cut-in and cut-out values of the selected turbine types. Here, the most frequent wind speed is 4 meters per second, also compare to Figure 5. However, since this value cannot lead to good LCOE values and is also not representative, as can also be seen in the formerly mentioned figure, as the main speed the average wind speed is chosen in the mentioned interval. That is about 5.2 meters per second.

This speed is needed to assign a value to the wind turbines in the wake calculation. Because potentially it is to be dealt with turbines of different types in the greedy algorithm, the calculation of the AEP is also based on this average wind speed: Instead of the calculation according to Formula 5, an approximation is used of the form

$$E_{\text{AEP}_{\text{gross}}} = (8760h + 6h) \cdot \sum_{j=1}^{n_{\text{turbines}}} \frac{u_{\text{current}}(j)}{u_{\text{cut-out}}(j)} \cdot P_{\text{out}}(j) . \quad (14)$$

Here,  $u_{\text{current}}(j)$  is the wind speed from the main wind direction at a turbine  $j$  with wake effect included,  $u_{\text{cut-out}}(j)$  is correspondingly the cut-out speed of turbine  $j$ , and  $P_{\text{out}}(j)$  is the electrical power that turbine  $j$  can generate.

Because the wake effect should be taken into account, when using Formula 5 the incoming wind speeds would have to be calculated, considering all possible wind directions and then wind speeds in each case, at each turbine for all of these instances, which would cost a lot of runtime.

For the individual costs per turbine, typical costs according to the data of the renewable energy consultants *BVG Associates*<sup>13</sup> are chosen. For the annual operation and maintenance costs and the expected lifetime of turbines, I use values from *THINK ACT*[4] and assume a discount/interest rate according to data from *IW Medien GmbH*<sup>14</sup>, which is part of the German Economic Institute *Institut der deutschen Wirtschaft*. An overview of the chosen values can be found in Table 4.

<sup>13</sup>Wind farm costs <https://guidetoanoffshorewindfarm.com/wind-farm-costs>. Accessed 24 Apr 2022.

<sup>14</sup>Interest rates long-term - in percent <https://www.deutschlandinzahlen.de/tab/welt/aussenwirtschaft0/zinsen/zinsen-langfristig>. Accessed 24 Apr 2022.

Variable	Description (see Section 3.4)	Assumed value
$c_{\text{project}}$	cost for project management	120 000 €
$c_{\text{substation}}$	cost of the substation	30 000 €
$c_{\text{cabling}}$	cable material cost and labor cost for laying the cables	170 000 €
$c_{\text{turbine}}$	cost of individual turbines	1 000 000 €
$c_{\text{foundation}}$	cost of individual turbine foundations	280 000 €
$c_{\text{MWoperation}}$	cost for operation of 1 MW	85 €
$r_{\text{rate}}$	discount/interest rate	0.3 %
$n_{\text{lifetime}}$	lifetime of the wind farm	10 years

Table 4: Variables used to calculate the LCOE, also see Section 3.4. Values are chosen according to *BVG Associates*, *THINK ACT*, and *IW Medien GmbH*.

The fact that here a constant turbine and foundation price for each of the turbine types are assumed and are not increased for larger turbines should not lead to any major distortions in the ratios of the results to each other: For this case study larger turbines lead to worse LCOE results anyway due to their characteristics related to the wind conditions prevailing. The reverse is true for the smaller turbines which can be seen in Table 6.

The cabling cost is also taken as a fixed value, since the positioning of a substation is not included in any of the algorithms and the value should not have a large impact on the final LCOE result relative to the other costs anyway.

For the ellipse-based approach, it is chosen to have 60 starting points for which optimal wind turbine placements are compared, thus there is a consideration of  $\frac{2 \cdot 180^\circ}{60} = 3^\circ$  - steps, see Section 3.1 and 4.2.1.

With this and the potential areas, the specific distribution of wind turbines is determined.

First, the following definition of the considered scenarios can be taken from Table 5. Accordingly, there is a comparison for all scenarios in Table 6 of the calculated optimal number of turbines, values of AEP and LCOE, see Section 3, and also the runtime of the optimization calculation.

The LCOE is always below a limit of 83 €/MW for the application of the greedy algorithm, which is set according to a study of Fraunhofer ISE [21].

Graphical representations of the specific turbine locations in the region for the various scenarios can be found in Appendix B.3.

### 5.3. Discussion of Results

In some of the scenarios (see Table 6: 1-6, 11, 23-26), each additional turbine planned, regardless of the wake effect, increases both the AEP, obviously, but also the LCOE. This applies to the planning of tall turbines of the types with large rotor diameters. Thus, for the given regional conditions, turbine types with smaller rotor diameters are apparently more suitable.

ID	Method	Minimal distance to houses	Turbine type(s)
1	ellipse-based	100	MM92
2	ellipse-based	200	MM92
3	ellipse-based	500	MM92
4	greedy	100	MM92
5	greedy	200	MM92
6	greedy	500	MM92
7	ellipse-based	600	MD77
8	ellipse-based	600	E-70 E4
9	greedy	600	MD77, E-70 E4
10	ellipse-based	600	GE 1.5sl
11	ellipse-based	600	MM82
12	greedy	600	GE 1.5sl, MM82
13	ellipse-based	600	W5200/750
14	ellipse-based	650	W5200/750
15	ellipse-based	600	D6-1000
16	ellipse-based	650	D6-1000
17	ellipse-based	600	NM 60/1000
18	ellipse-based	650	NM 60/1000
19	greedy	600	W5200/750, D6-1000, NM 60/1000
20	greedy	650	W5200/750, D6-1000, NM 60/1000
21	ellipse-based	600	E-82 E2
22	ellipse-based	650	E-82 E2
23	ellipse-based	600	MM82
24	ellipse-based	650	MM82
25	ellipse-based	600	Test Turbine
26	ellipse-based	650	Test Turbine
27	greedy	600	E-82 E2, MM82, Test Turbine
28	greedy	650	E-82 E2, MM82, Test Turbine

Table 5: Initial values for the scenarios considered in Herzogenrath. The minimum distances to houses, as well as the turbine types are chosen arbitrarily, for turbine properties see Appendix 9.

<b>ID</b>	<b>Number of turbines</b> (greedy: total number, then distribution to types)	<b>AEP</b> (MW)	<b>LCOE</b> (€/MW)	<b>Runtime</b> (min:sec)
1	500 MM92	1886.68	34501.50	15:35
2	272 MM92	1026.36	34515.95	14:09
3	17 MM92	64.15	34991.38	8:42
4	2: 2 MM92	24816527.03	80.00	41:19
5	2: 2 MM92	24816527.03	80.00	14:00
6	2: 2 MM92	24816527.03	80.00	0:36
7	5 MD77	16980.14	40.27	0:03
8	5 E-70 E4	13317.76	51.36	0:03
9	41: 39 MD77, 2 E-70 E4	133464849.1	56.05	13:58
10	5 GE 1.5sl	13584.11	50.34	0:04
11	4 MM82	14.49	38166.17	0:03
12	43: 43 GE 1.5sl, 0 MM82	106401159.29	68.85	15:44
13	8 W5200/750	13584.11	79.06	0:03
14	3 W5200/750	5094.04	83.06	0:02
15	6 D6-1000	11812.27	68.89	0:05
16	3 D6-1000	5906.13	71.65	0:03
17	6 NM 60/1000	13584.11	59.91	0:04
18	3 NM 60/1000	6792.06	62.30	0:02
19	56: 1 W5200/750, 0 D6-1000, 55 NM 60/1000	144842179.06	62.25	44:45
20	8: 0 W5200/750, 0 D6-1000, 8 NM 60/1000	27701517.37	81.93	0:02
21	4 E-82 E2	10654.20	51.97	0:07
22	2 E-82 E2	5327.10	55.02	0:04
23	4 MM82	14.49	38166.17	0:03
24	2 MM82	7.24	40411.23	0:04
25	2 Test Turbine	30.19	9698.71	0:11
26	2 Test Turbine	30.19	9698.71	0:03
27	36: 36 E-82 E2, 0 MM82, 0 Test Turbine	88120909.52	72.81	17:48
28	7: 7 E-82 E2, 0 MM82, 0 Test Turbine	27130434.55	76.57	0:11

Table 6: Results of different optimization methods for the scenarios in Herzogenrath.  
For information on the scenarios considered, see Table 5.

This fact also leads to the particularly large differences in the LCOE results between the ellipse-based and greedy algorithm and already reveals a weakness of the former: Because the LCOE is completely neglected during the execution of the algorithm, the rapid increase of it by each additional planned turbine does not lead to any consequences.

On the other hand, very good LCOE values are achieved with the mentioned more suitable turbine types, because leaving the elliptical area around each turbine free very much restricts wake and therefore hardly affects the good LCOE that each individual turbine has for itself in the region under consideration. Whether this is seen as an advantage or disadvantage probably depends on the point of view. With the better LCOE compared to the greedy algorithm, there are fewer planned turbines, and thus a lower AEP. In addition, the limit value of the LCOE for the greedy algorithm could also be adapted in such a way that it calculates a wind turbine planning for the same conditions. In this case, of course, the runtime would have to be taken into account in each case and thus it would have to be decided how much sense this procedure would make, especially depending on the area size.

The runtime of the ellipse-based algorithm depends on the number of iterations for the calculation of the distance coefficient in the refinement step, see Section 4.1.2. Values for the scenarios for final iterations and coefficients can be found in Table 7. As expected, correlations between turbine types and these values are not found. Indeed, no property of the turbine type affects the coefficient, but only the number of turbines planned.

The greedy algorithm, on the other hand, always needs exactly as many iterations as planned turbines or one more: Sometimes the limit set by the maximum LCOE is not reached at all when the greedy algorithm is executed. That can happen if the case occurs beforehand that each newly planned turbine would lead to such a large wake effect on at least one other turbine in the region that no more energy could be generated at the latter. The reasons for terminating the greedy algorithm for each of the considered scenarios can be found in Table 8. This again shows that for the considered area turbine types with smaller rotor diameters lead to significantly better LCOE values.

In contrast, it can be observed that for the cases with unsuitable turbine types (compare scenarios 1 to 3 with scenarios 4 to 6), the positioning is chosen in such a way that the turbines do not generate wake for each other. The large distances are possible because this is a reaction to the rapidly increasing LCOE and the wind turbine planning ends after positioning only a few turbines.

In addition, the most obvious disadvantage of the greedy algorithm becomes very clear in Table 6: The larger the considered area, the longer the algorithm needs to find the optimal values for each newly planned wind turbine. This is because the algorithm iterates over all free squares of the region for each turbine type in each step, see Algorithm 3. Thus, the runtime can be very high if the area is very large or many wind turbines can be scheduled until the LCOE maximum is reached. This is also the reason for the chosen distances to buildings in the scenarios for scheduling smaller wind turbine types: Because so many are planned here, the calculations would take several

Scenario ID	Number of iterations	Final coefficient $\xi$
1	6	1.00
2	6	1.00
3	6	1.00
7	6	1.00
8	6	1.09
10	6	1.00
11	5	1.01
13	6	1.00
14	8	1.49
15	7	1.08
16	7	1.25
17	7	1.11
18	8	1.29
21	8	1.23
22	13	1.98
23	5	1.01
24	11	1.63
25	12	1.88
26	7	1.08

Table 7: More details on the optimization process with the **ellipse-based** approach, see Algorithm 1.

hours to days even for about an increase of the area from 136 to 670 squares when downsizing to a house distance of only 500 metres.

Furthermore, it is noticeable that for the scenarios presented, the greedy algorithm hardly uses the fact that different turbine types are available. One turbine type is always clearly preferred, whereas only a minority of other turbine types or even no turbine at all are planned. This is certainly due to the fact that the wind conditions of the considered region are, as already mentioned, very unfavorable for high turbines with large rotor diameters. Presumably, the greedy algorithm would provide for the most distribution between types if large turbines were most advantageous. So scheduling these would result in more and more wake on the area that the "gaps" then created would have to be filled with smaller turbines for further improvement in LCOE results.

Scenario ID	Termination reason
4	Reaching the maximum LCOE
5	Reaching the maximum LCOE
6	Reaching the maximum LCOE
9	Another turbine led to too much wake
12	Another turbine led to too much wake
19	Another turbine led to too much wake
20	Reaching the maximum LCOE
27	Another turbine led to too much wake
28	Reaching the maximum LCOE

Table 8: More details on the optimization process with the **greedy** approach, see Algorithm 3.

## 6. Conclusion and Future Work

The optimization of wind farms for the generation of renewable energy is currently a topic of high interest as already described in the introduction. The present work adds to this a further comparison of two different algorithmic approaches. These differ in terms of the number of turbine types considered and the economic data taken into account, as well as modeled data on the influence of wakes of the turbines on each other.

I found that for the example region Herzogenrath, good economic results are possible with both the multi-step ellipse-based and the greedy optimization algorithm. In certain cases, however, both algorithms reach limits caused by their approaches. This applied in the case of the ellipse-based approach with respect to economic factors and in particular the LCOE, and in the case of the greedy approach with respect to run-times.

In general, wind farm planning is dependent on many regional factors in the areas of topography, weather, and legal regulations regarding building permits.

In particular, I observed that the spacing requirements alone can constrain the amount of land that can be used for planning, depending on the type of turbine, and that wind data and the selection of turbine types used are significant factors in the suitability of different types of wind turbines.

Thus, it is partly useful to use different turbine types mixed and partly better to consider only one turbine type at a time. The general superiority of the greedy algorithm observed by Chen et al. [9] could not be further supported in my specific comparison and example.

## 6.1. Future Work

- develop a method to be able to estimate in advance which algorithm will produce better results than the other one under certain conditions with respect to a clearly defined goal
- observations on the behavior of the algorithms with more variability in parameter selection, such as for example more or less starting points in the ellipse-based algorithm or very specific and individualized turbine costs in the greedy approach
- consideration of all wind directions instead of summarizing on  $0^\circ$  to  $180^\circ$ , see Section 3.1, to consider neighboring already existing turbines
- in case of ellipse-based algorithm take several or even all configurations into the refinement step and do not already discard all except one
- test the optimizations in other regions, for example with different wind conditions
- many other factors can be included in the optimization, as should have already emerged from Section 1.1...
- topicality of the subject continues to cause more in-depth discussion: for example, repowering is currently to be promoted more in Germany (i.e., replacing old wind turbines with newer, more efficient ones) → consider promising approaches to optimization in present algorithms

## A. Turbine Properties

<b>Turbine type</b>	<b><math>H</math> in meters</b>	<b><math>D</math> in meters</b>	<b>cut-in speed</b>	<b>cut-out speed</b>
D6-1000	91.5	62	2.5	23
E-70 E4	113	71	2.5	34
E-82 E2	138	82	2	34
GE 1.5sl	100	77	3.5	25
MD77	111.5	77	3	20
MM82	120	100	3.5	25
MM92	100	92	3	24
NM 60/1000	80	60	3	20
Test Turbine	150	150	4	15
W5200/750	45	52	3.5	20

Table 9: Hub heights, rotor diameters, cut-in speeds, and cut-out speeds of the turbine types used for the specific comparisons.

## B. Plots

All following plots were created during the execution of the respective program. The numbers at the axes refer to the internal numbering of the squares as described in Section 2 and thus correspond to a Cartesian coordinate system. The distance between two points corresponds accordingly to 20 meters.

### B.1. Plots of Exemplary Ellipse-Based Optimization

In each case, the red dot represents the position of the newly added turbine and the blue dots indicate the turbine locations planned in the previous steps.

The procedure of turbine placement is done according to Algorithm 1, compare also with the plot of the corresponding potential area in Figure 29.

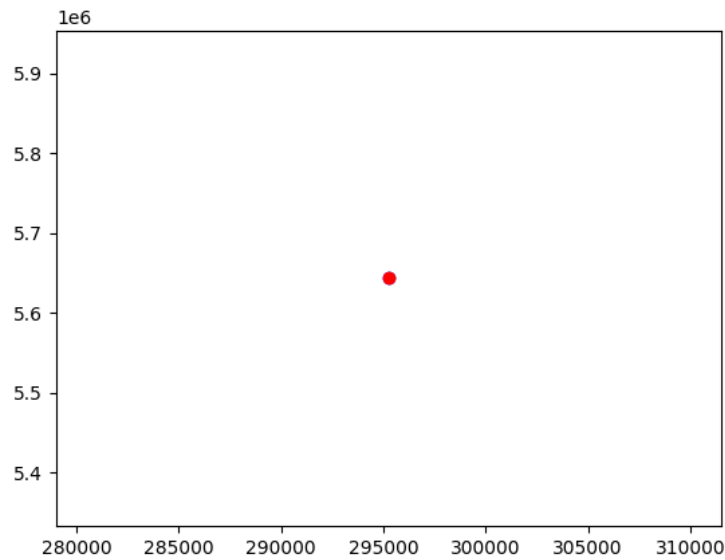


Figure 10: Step 1 of finding an initial turbine setup for scenario 3.

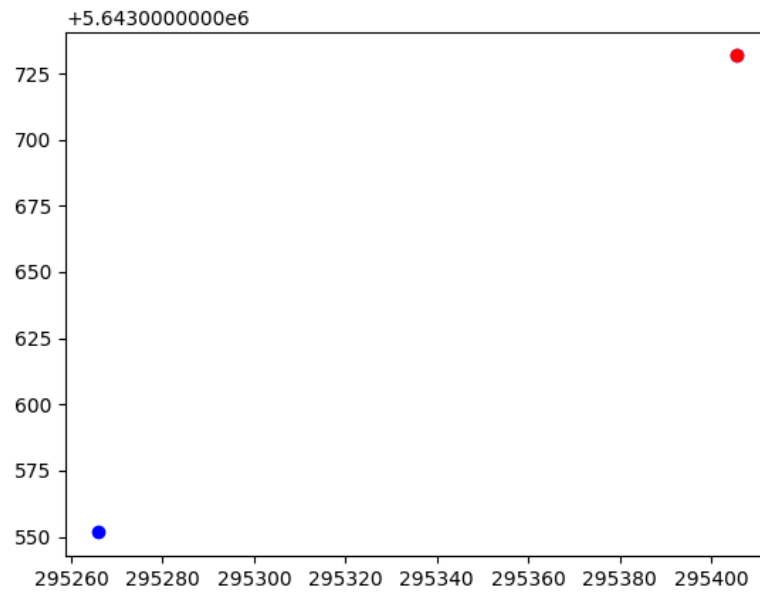


Figure 11: Step 2 of finding an initial turbine setup for scenario 3.

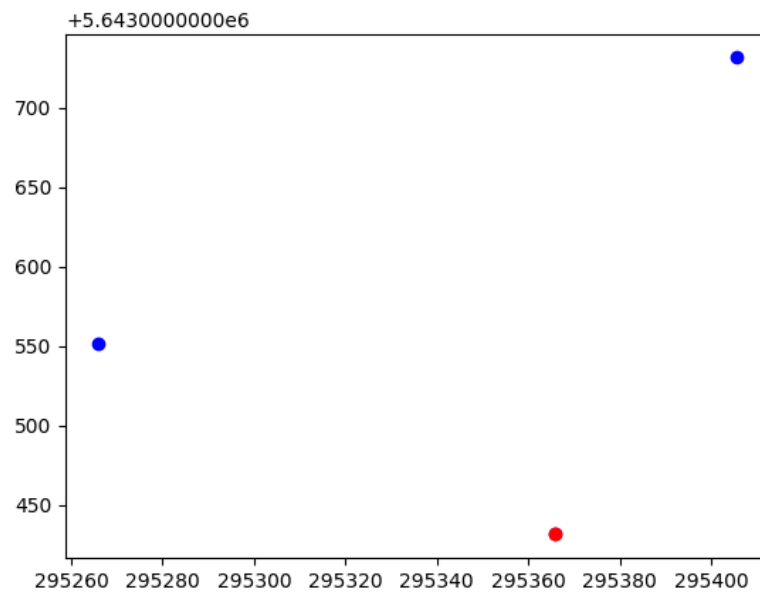


Figure 12: Step 3 of finding an initial turbine setup for scenario 3.

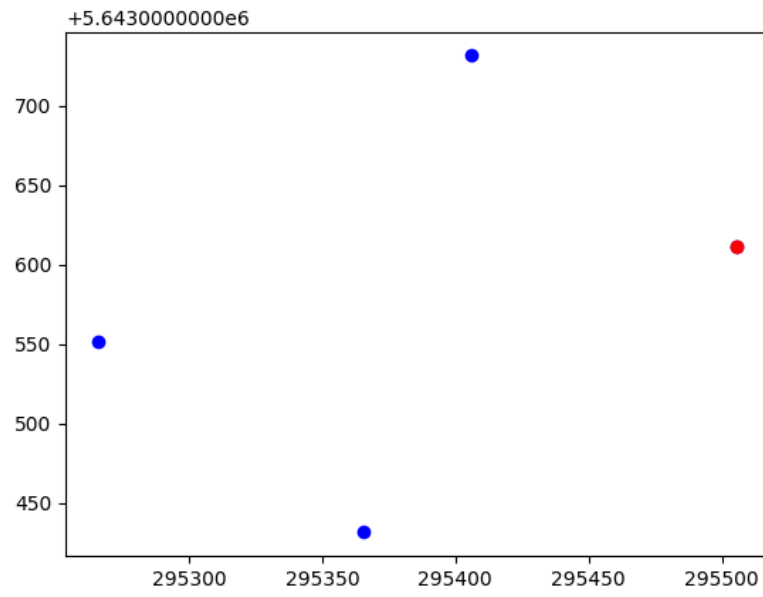


Figure 13: Step 4 of finding an initial turbine setup for scenario 3.

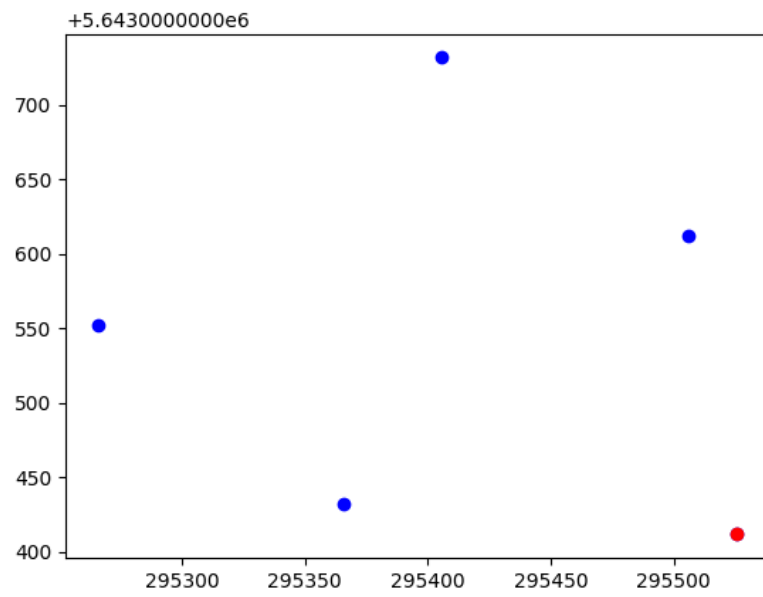


Figure 14: Step 5 of finding an initial turbine setup for scenario 3.

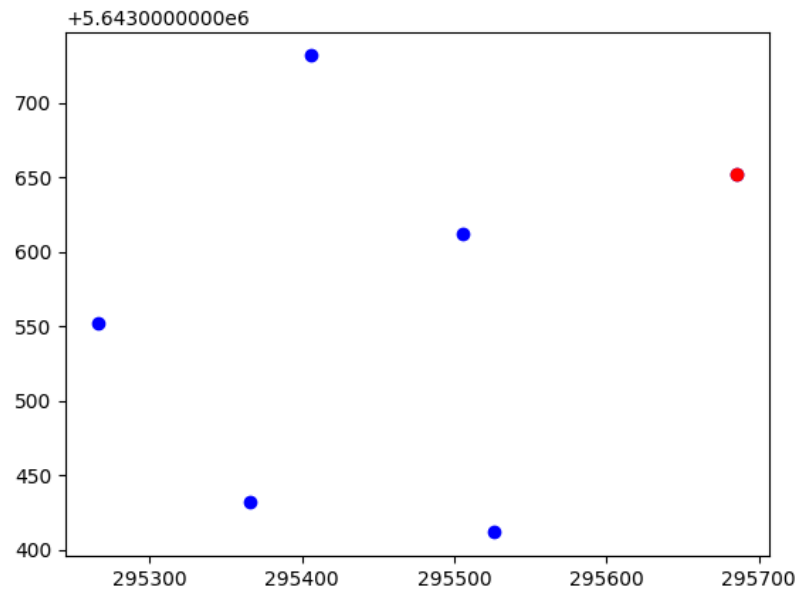


Figure 15: Step 6 of finding an initial turbine setup for scenario 3.

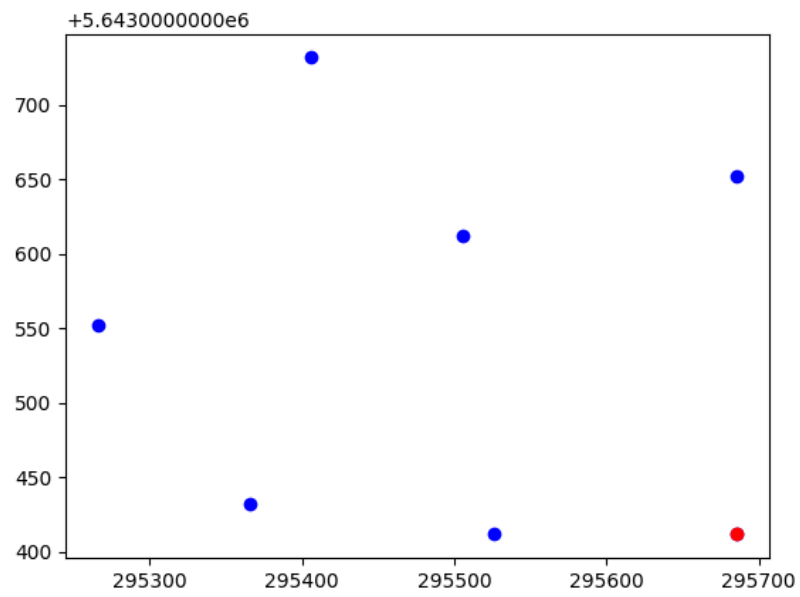


Figure 16: Step 7 of finding an initial turbine setup for scenario 3.

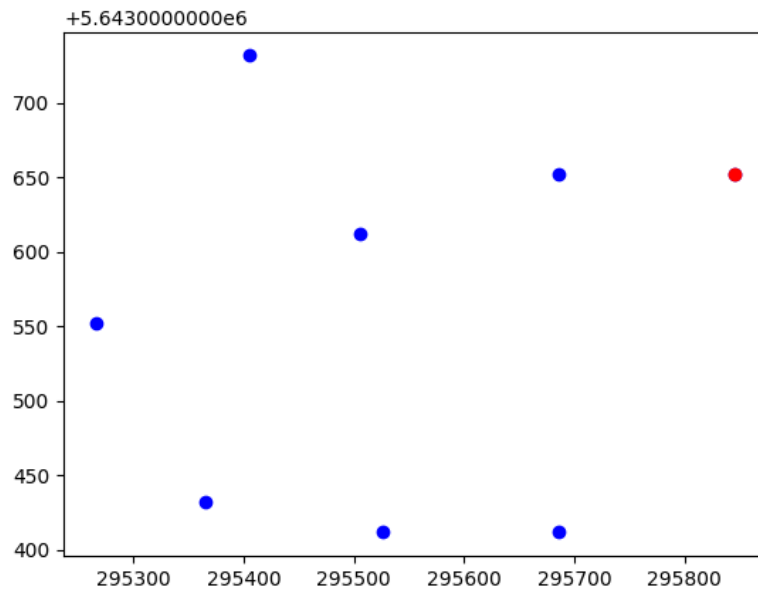


Figure 17: Step 8 of finding an initial turbine setup for scenario 3.

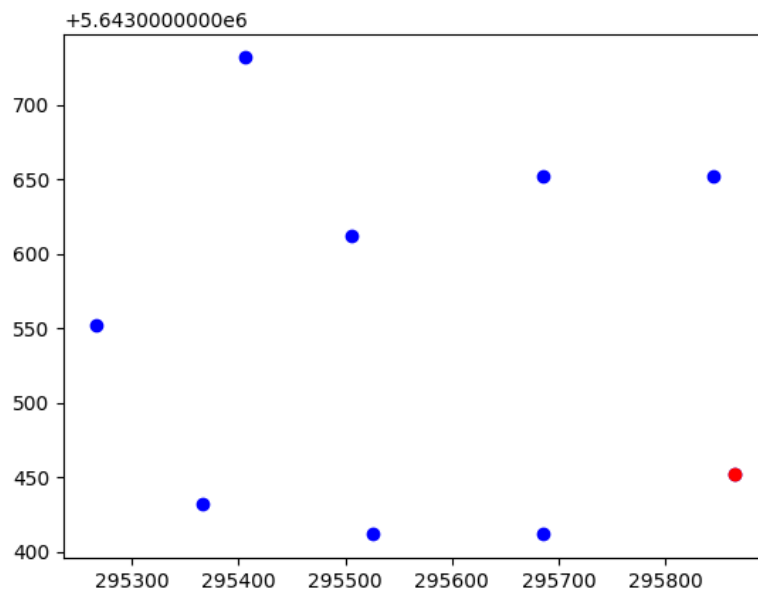


Figure 18: Step 9 of finding an initial turbine setup for scenario 3.

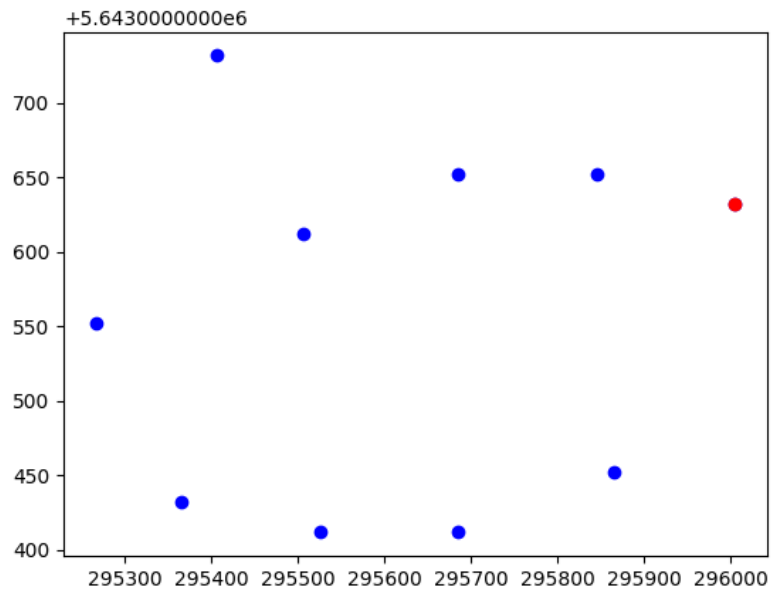


Figure 19: Step 10 of finding an initial turbine setup for scenario 3.

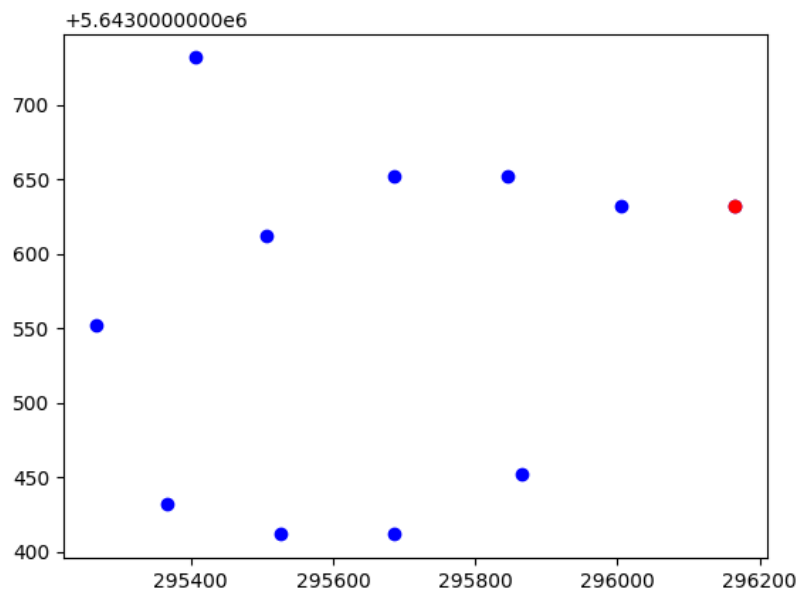


Figure 20: Step 11 of finding an initial turbine setup for scenario 3.

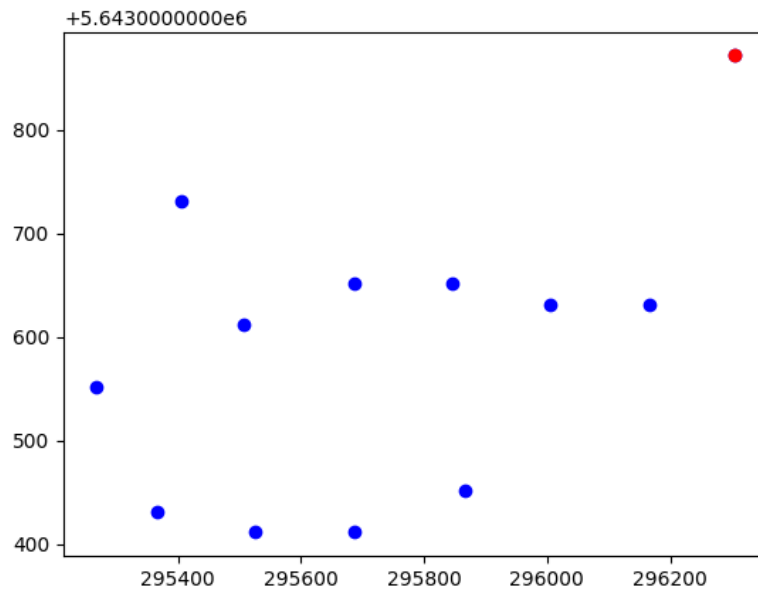


Figure 21: Step 12 of finding an initial turbine setup for scenario 3.

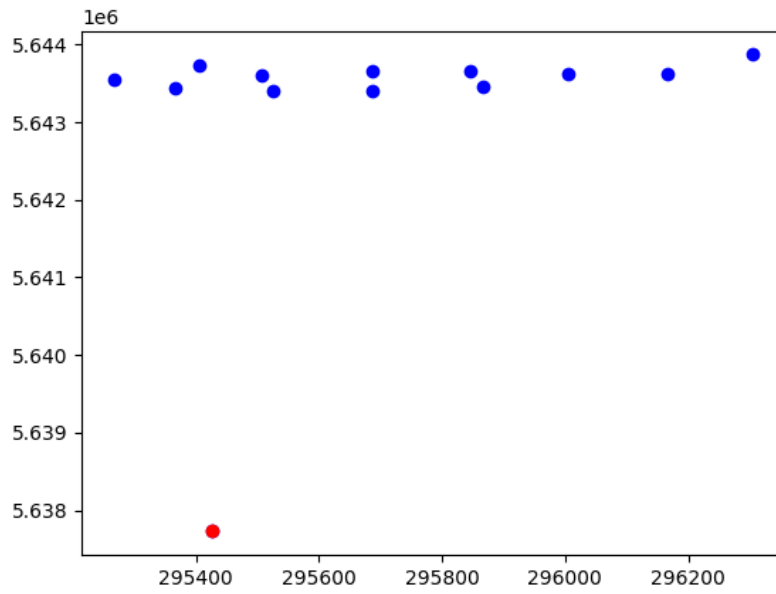


Figure 22: Step 13 of finding an initial turbine setup for scenario 3.

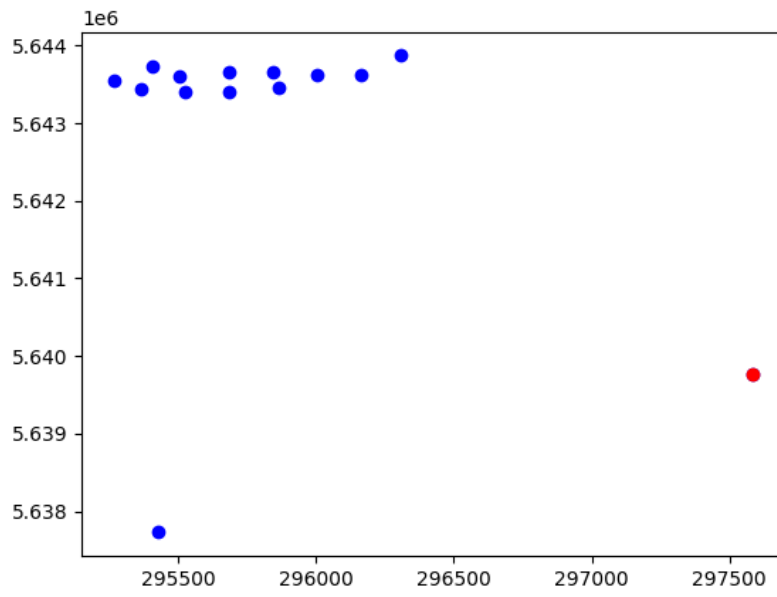


Figure 23: Step 14 of finding an initial turbine setup for scenario 3.

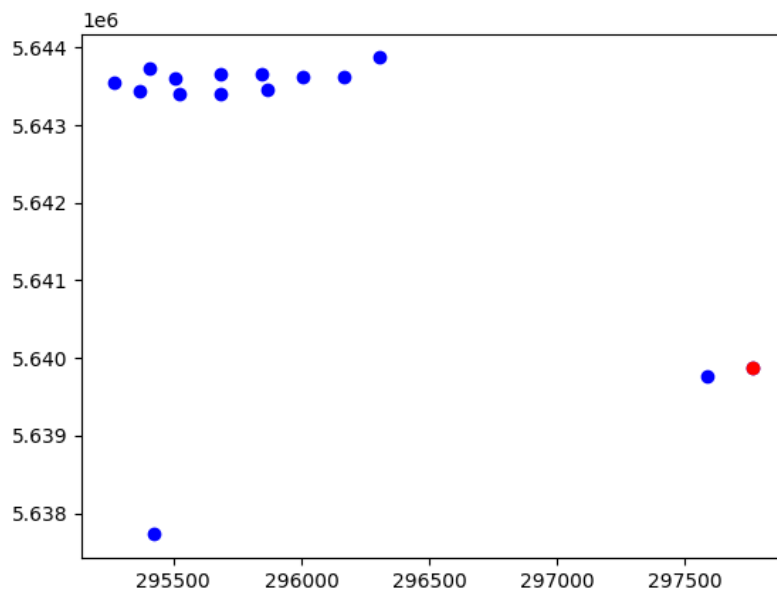


Figure 24: Step 15 of finding an initial turbine setup for scenario 3.

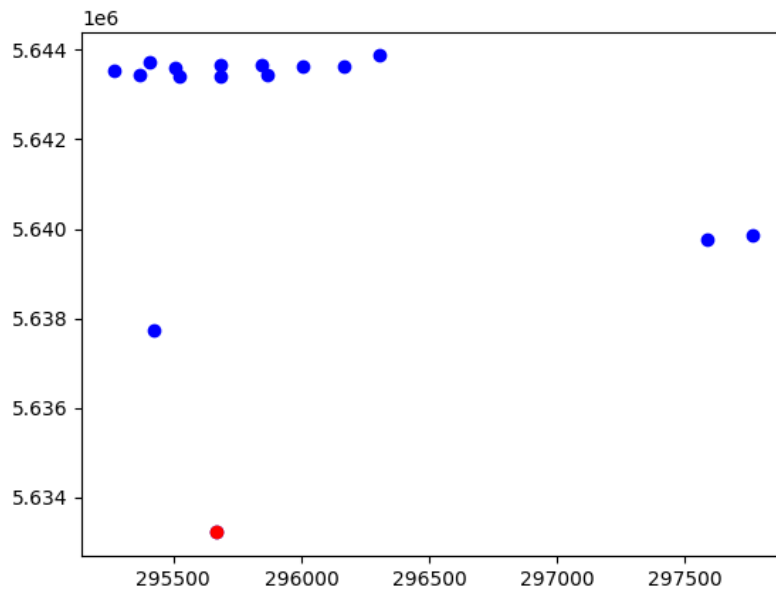


Figure 25: Step 16 of finding an initial turbine setup for scenario 3.

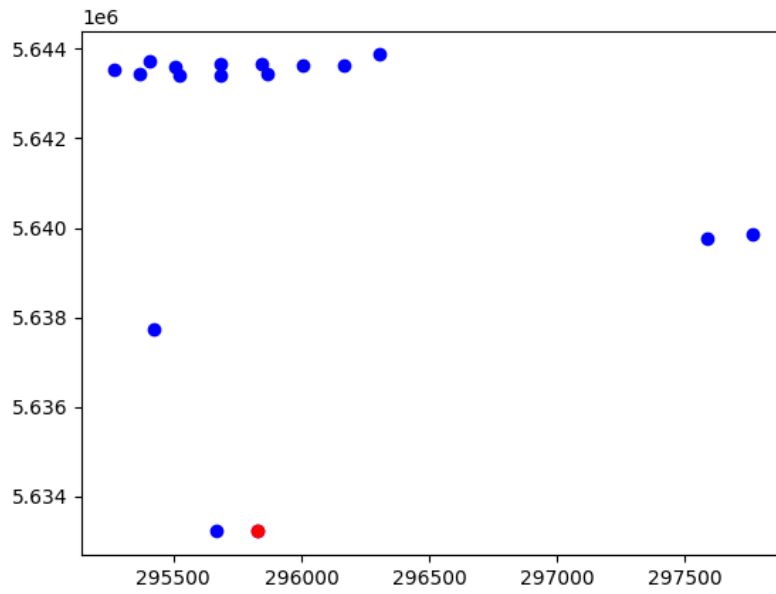


Figure 26: Step 17 of finding an initial turbine setup for scenario 3.

## B.2. Plots of Potential Area

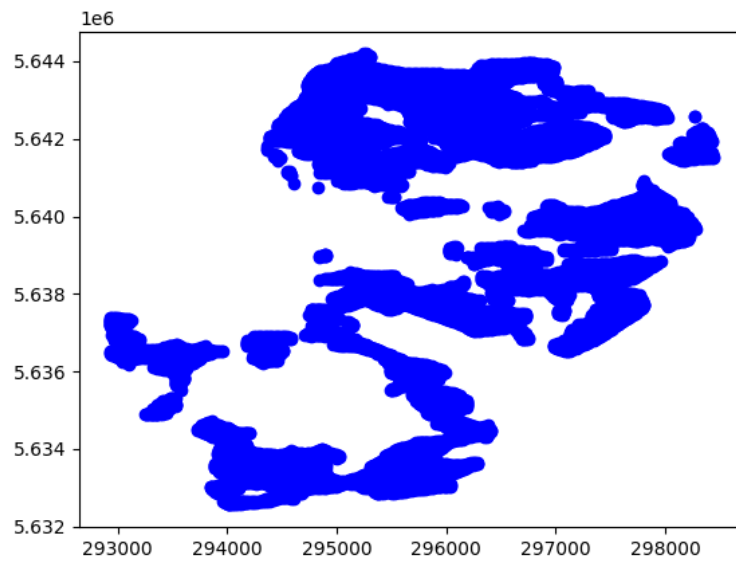


Figure 27: Potential area for turbine type MM92 and a minimum distance to houses of 100 meters.

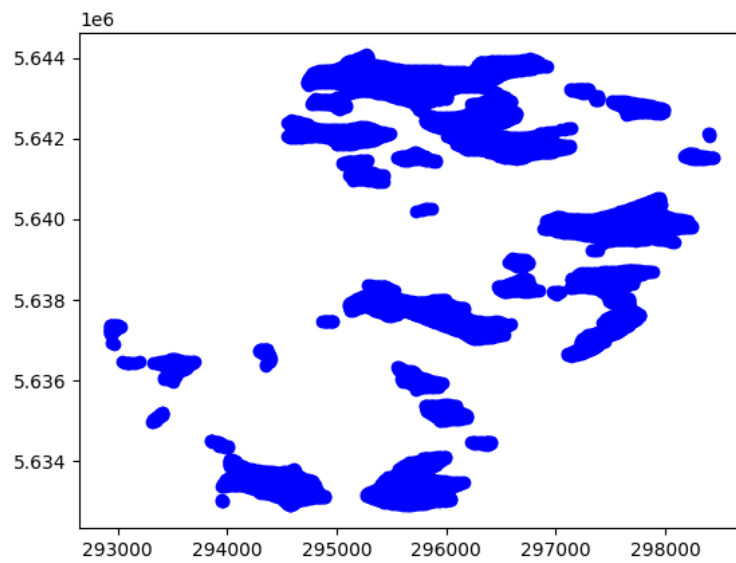


Figure 28: Potential area for turbine type MM92 and a minimum distance to houses of 200 meters.

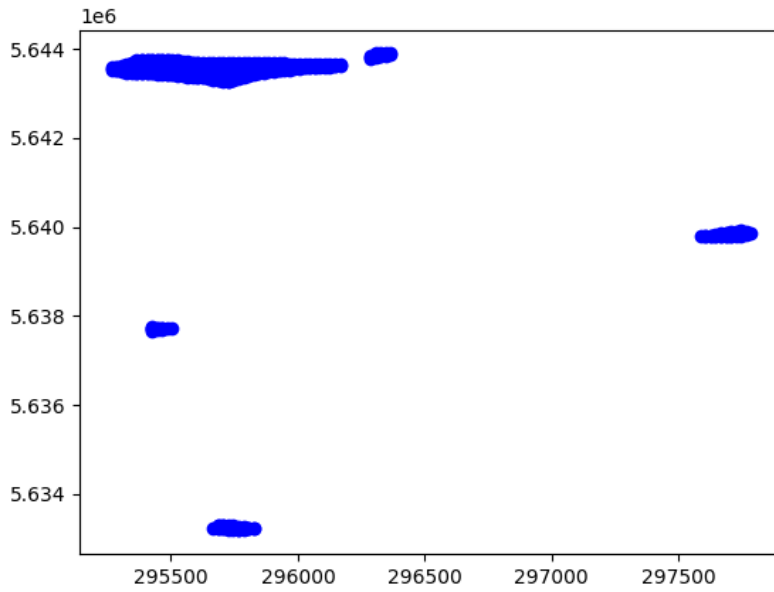


Figure 29: Potential area for turbine type MM92 and a minimum distance to houses of 500 meters.

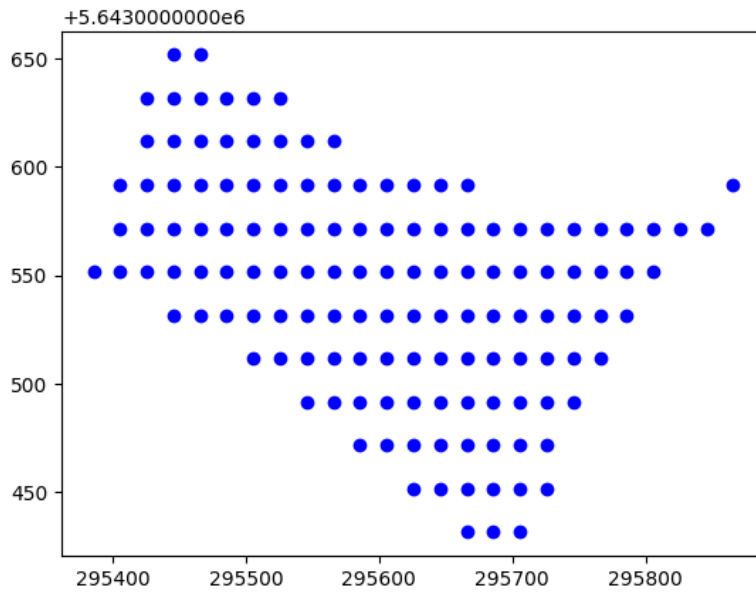


Figure 30: Potential area for turbine types MD77, E-70 E4, GE 1.5sl, MM82, W5200/750, D6-1000, NM 60/1000, E-82 E2, Test Turbine and a minimum distance to houses of 600 meters.

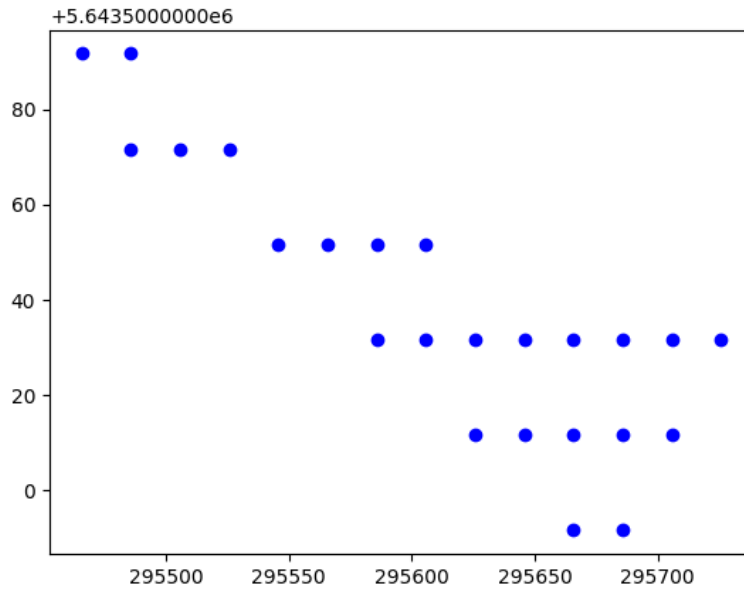


Figure 31: Potential area for turbine types W5200/750, D6-1000, NM 60/1000, E-82 E2, MM82, Test Turbine and a minimum distance to houses of 650 meters.

### B.3. Plots of Final Turbine Positioning

#### B.3.1. Ellipse-Based Algorithm

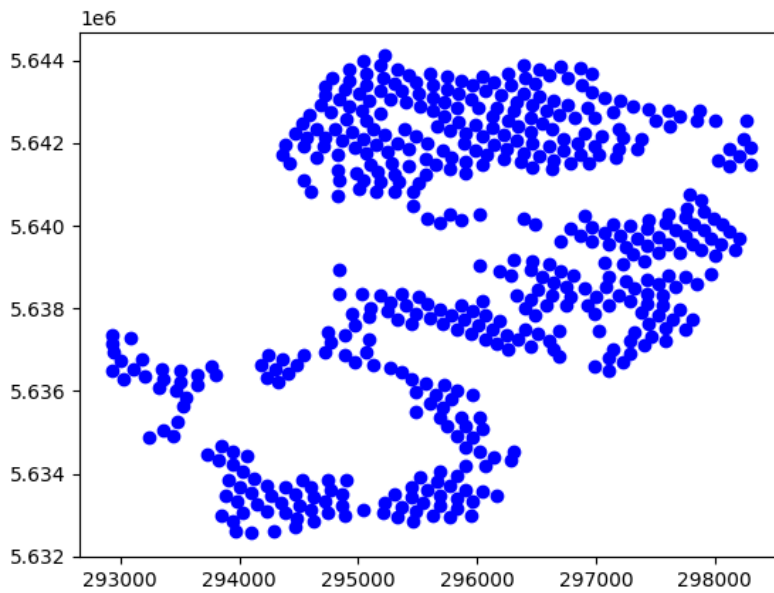


Figure 32: Turbines positions of Scenario 1.

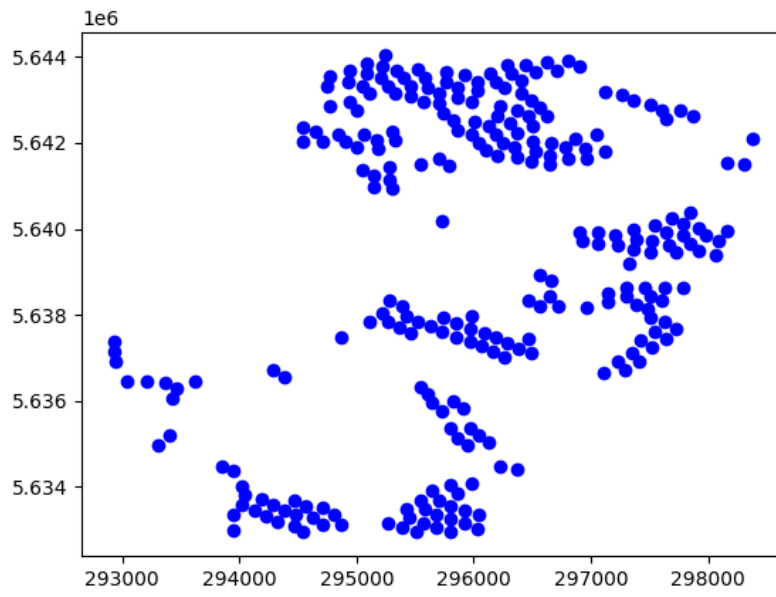


Figure 33: Turbines positions of Scenario 2.

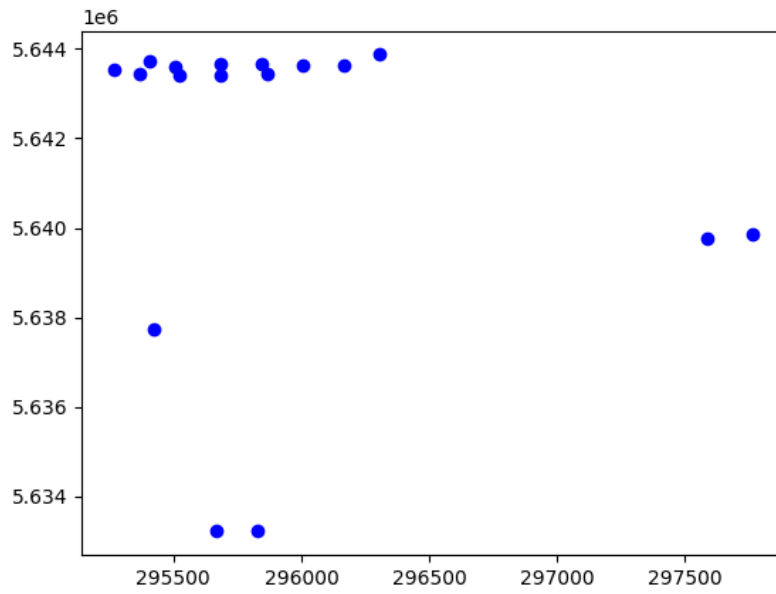


Figure 34: Turbines positions of Scenario 3.

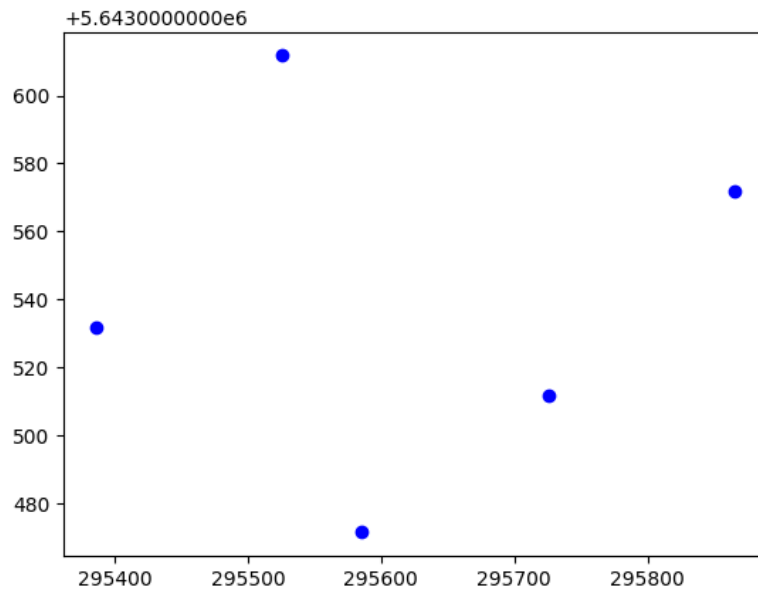


Figure 35: Turbines positions of Scenario 7, 8, 10.

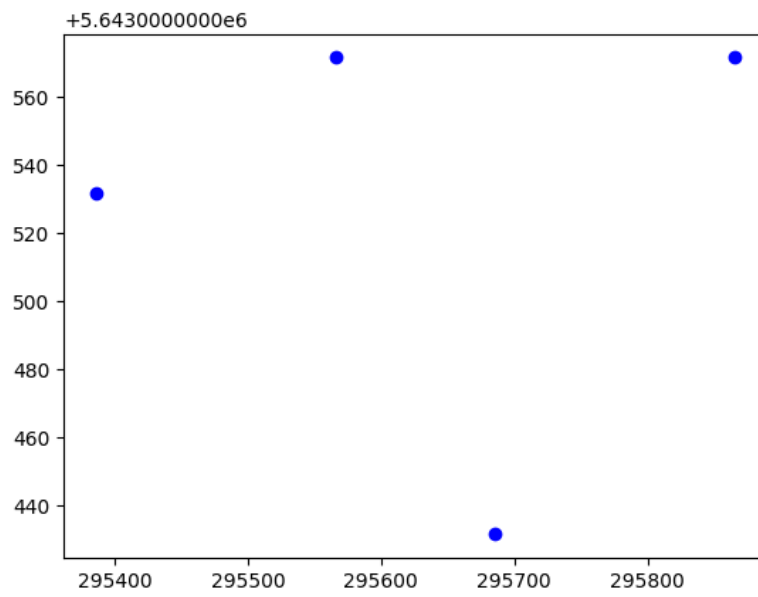


Figure 36: Turbines positions of Scenario 11, 21, 23.

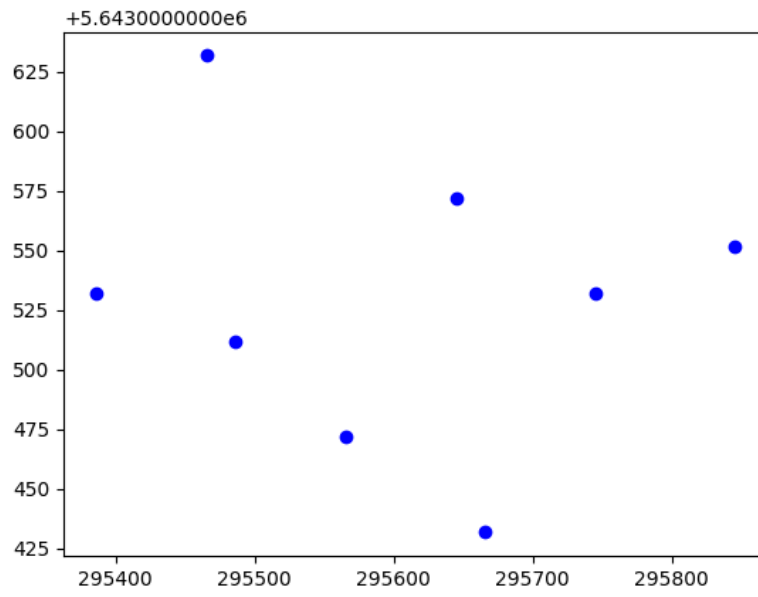


Figure 37: Turbines positions of Scenario 13.

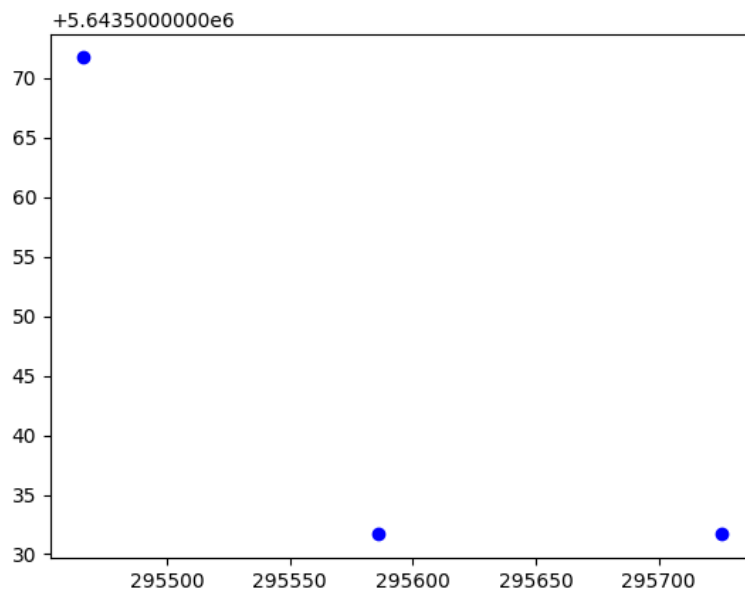


Figure 38: Turbines positions of Scenario 14, 16, 18.

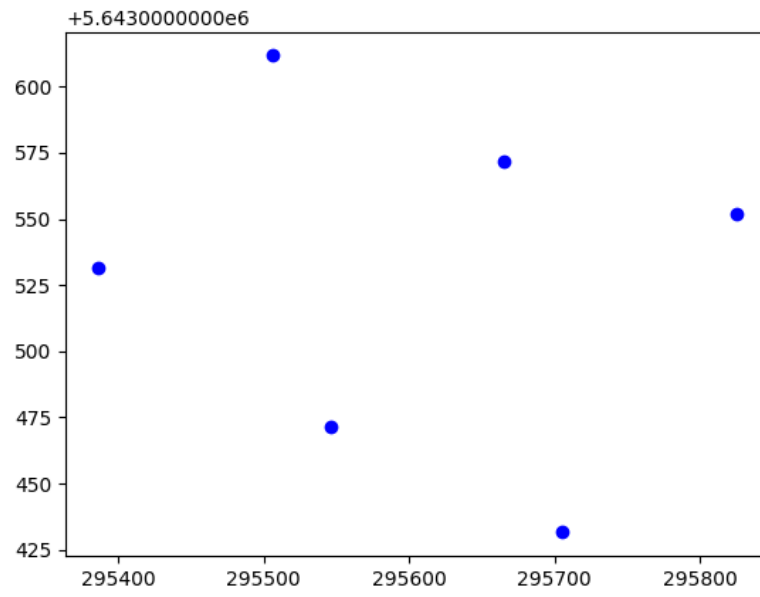


Figure 39: Turbines positions of Scenario 15, 17.

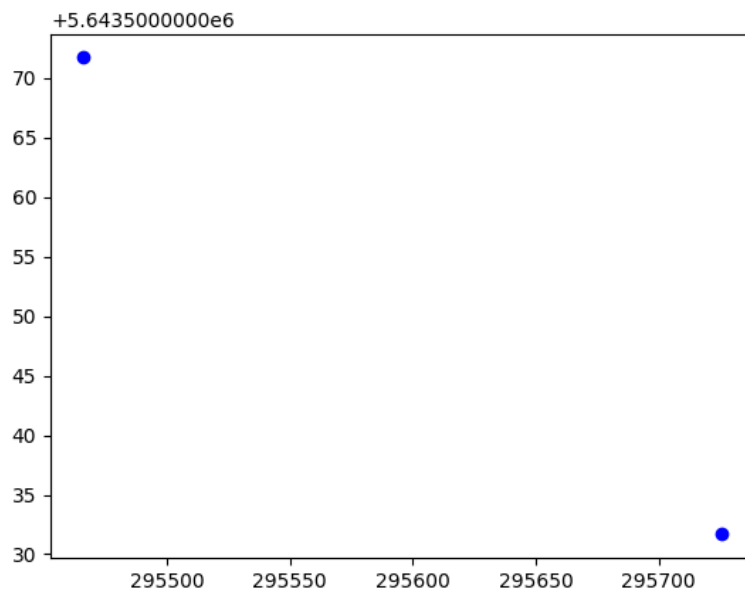


Figure 40: Turbines positions of Scenario 22, 24, 26.

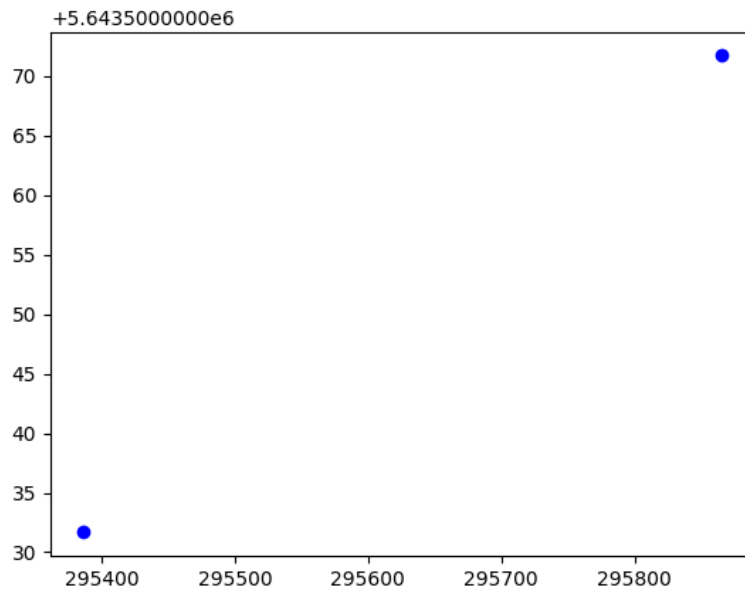


Figure 41: Turbines positions of Scenario 25.

s

### B.3.2. Greedy Algorithm

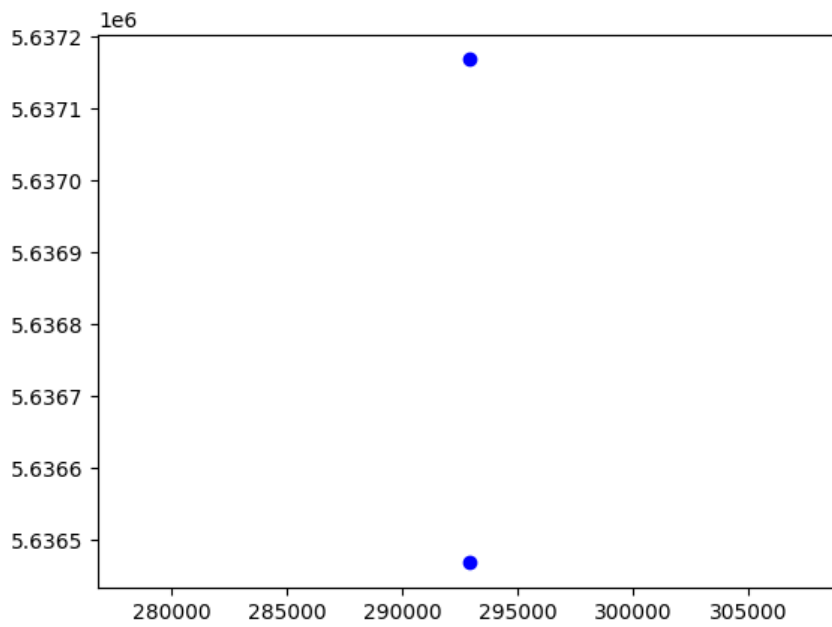


Figure 42: Turbines positions of Scenario 4, 5.

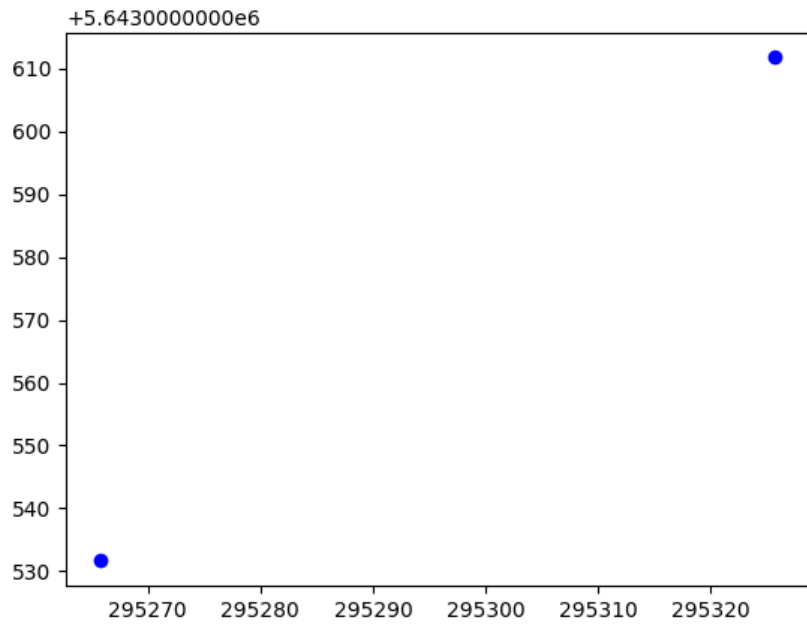


Figure 43: Turbines positions of Scenario 6.

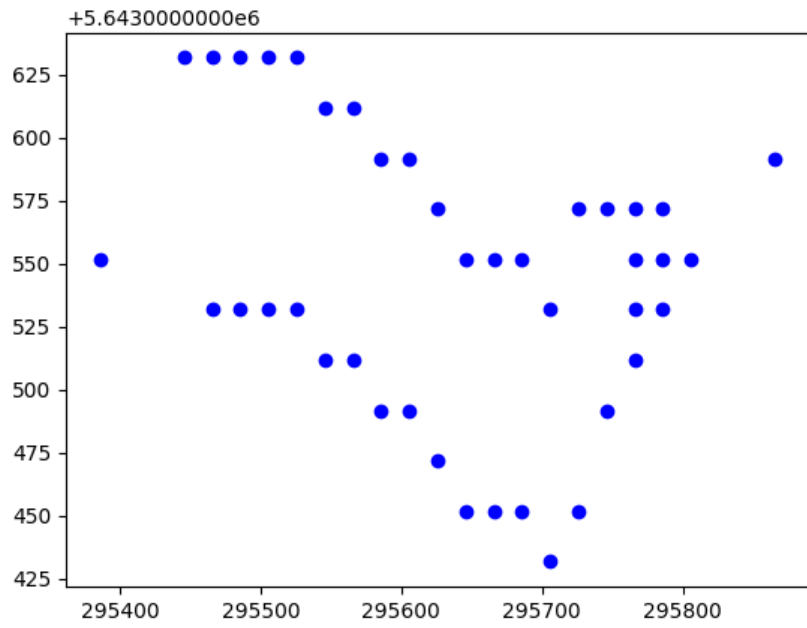


Figure 44: Turbines positions of Scenario 9.

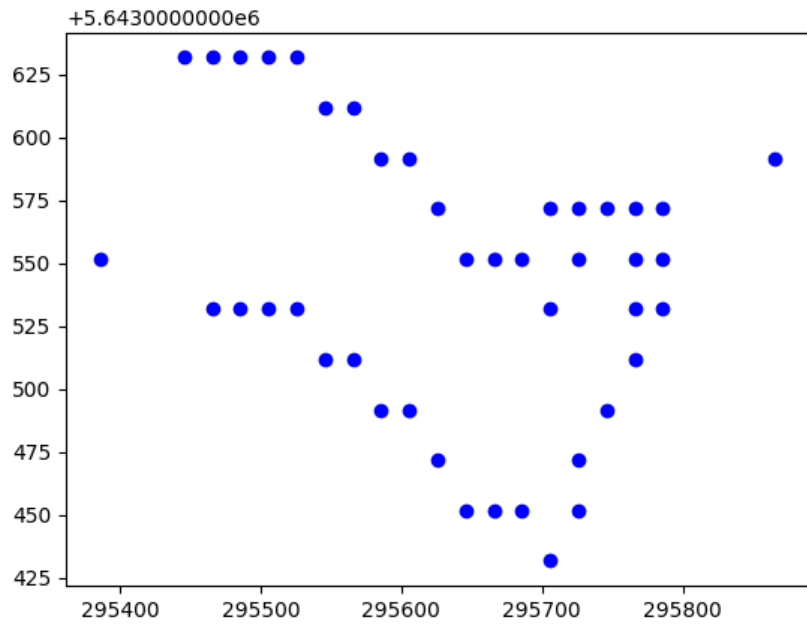


Figure 45: Turbines positions of Scenario 12.

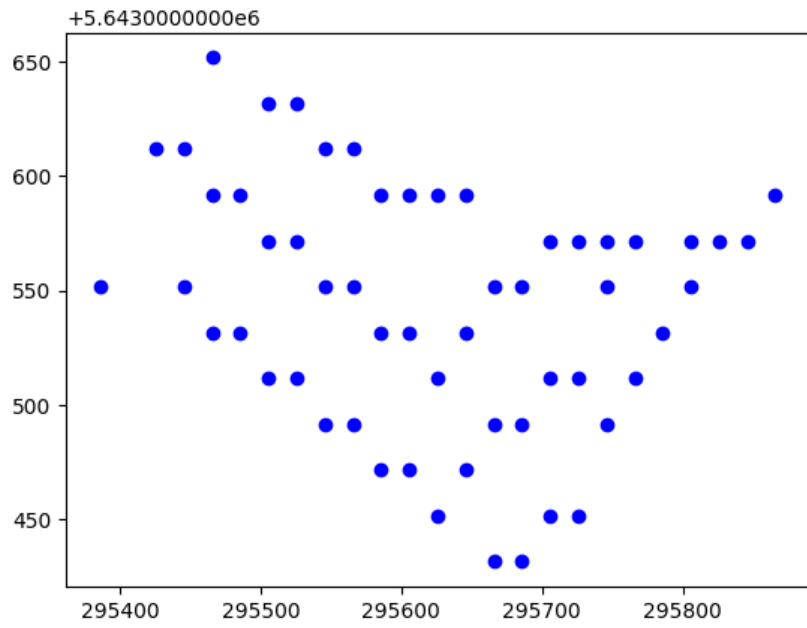


Figure 46: Turbines positions of Scenario 19.

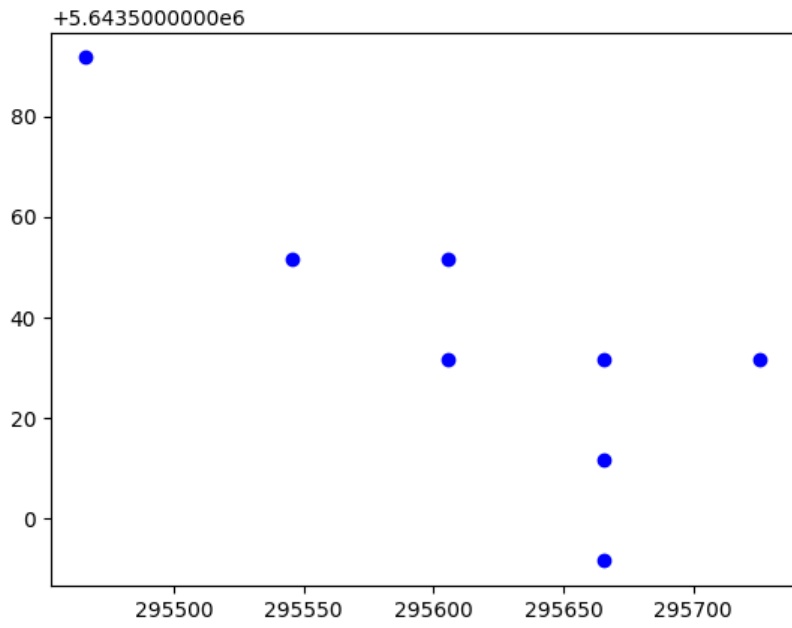


Figure 47: Turbines positions of Scenario 20.

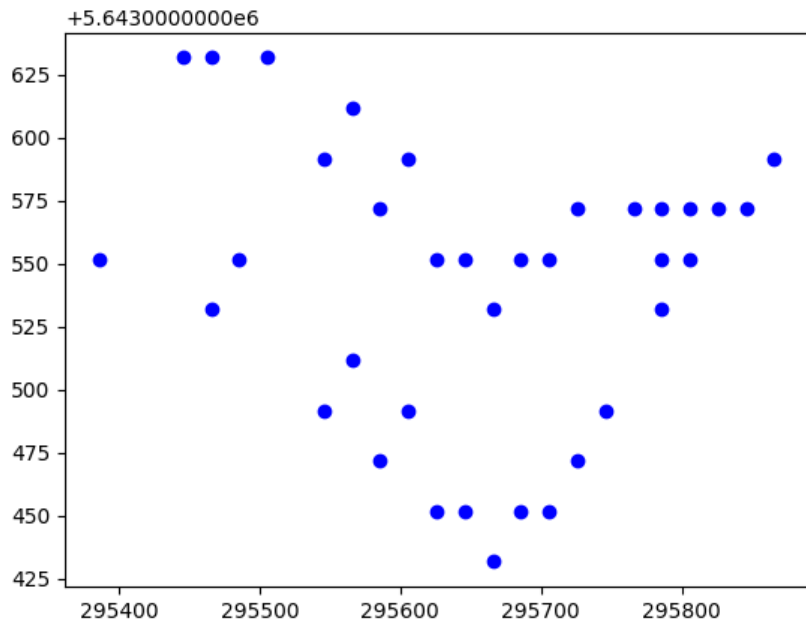


Figure 48: Turbines positions of Scenario 27.

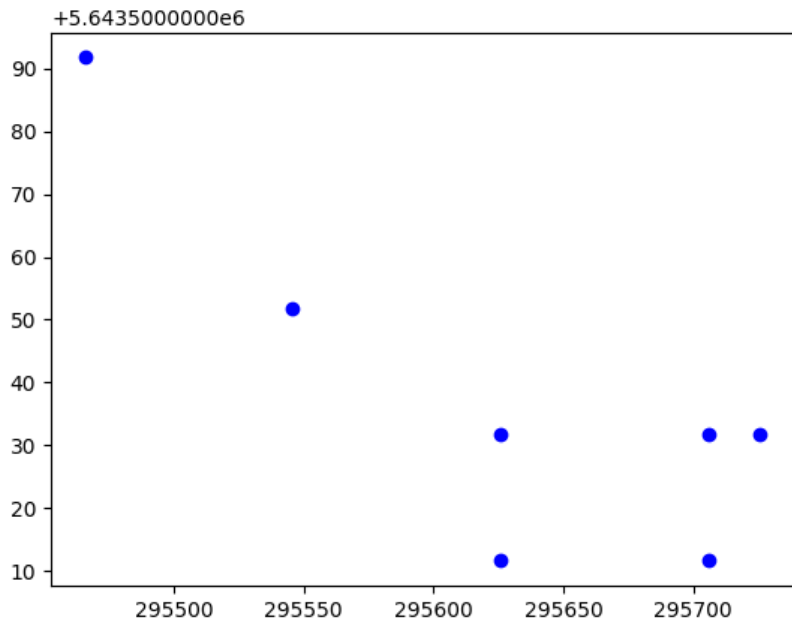


Figure 49: Turbines positions of Scenario 28.

## References

- [1] Sahar Ammous, Mariam Jebali, Nahla Ben Halima, Hsan Hadj Abdallah, and Abdelmajid Oualha. Development of a genetic algorithm for maximizing wind power integration rate into the electric grid. *Journal of Renewable and Sustainable Energy*, 11(2):023303, Mar 2019. ISSN 1941-7012. doi: 10.1063/1.5068736.
- [2] U. Aytun Ozturk and Bryan A. Norman. Heuristic methods for wind energy conversion system positioning. *Electric Power Systems Research*, 70(3):179–185, Aug 2004. ISSN 0378-7796. doi: 10.1016/j.epsr.2003.12.006.
- [3] Jagdish Chand Bansal, Pushpa Farswan, and Atulya K. Nagar. Design of wind farm layout with non-uniform turbines using fitness difference based bbo. *Engineering Applications of Artificial Intelligence*, 71:45–59, May 2018. ISSN 0952-1976. doi: 10.1016/j.engappai.2018.02.007.
- [4] Roland Berger. Windkraft Onshore - Neue Spielregeln für einen reifen Markt, Jan 2016.
- [5] Marc Calaf, Charles Meneveau, and Johan Meyers. Large eddy simulation study of fully developed wind-turbine array boundary layers. *Physics of Fluids*, 22(1): 015110, Jan 2010. ISSN 1089-7666. doi: 10.1063/1.3291077.
- [6] K. Chen, M. X. Song, Z. Y. He, and X. Zhang. Wind turbine positioning optimization of wind farm using greedy algorithm. *Journal of Renewable and Sustainable Energy*, 5(2):023128, Mar 2013. ISSN 1941-7012. doi: 10.1063/1.4800194.
- [7] K. Chen, M. X. Song, Z. Y. He, and X. Zhang. Wind turbine positioning optimization of wind farm using greedy algorithm. *Journal of Renewable and Sustainable Energy*, 5(2):023128, Mar 2013. ISSN 1941-7012. doi: 10.1063/1.4800194.
- [8] K. Chen, M.X. Song, and X. Zhang. The iteration method for tower height matching in wind farm design. *Journal of Wind Engineering and Industrial Aerodynamics*, 132:37–48, Sep 2014. ISSN 0167-6105. doi: 10.1016/j.jweia.2014.06.017.
- [9] K. Chen, M.X. Song, X. Zhang, and S.F. Wang. Wind turbine layout optimization with multiple hub height wind turbines using greedy algorithm. *Renewable Energy*, 96:676–686, Oct 2016. ISSN 0960-1481. doi: 10.1016/j.renene.2016.05.018.
- [10] Le Chen and Erin MacDonald. A new model for wind farm layout optimization with landowner decisions. *Volume 5: 37th Design Automation Conference, Parts A and B*, Jan 2011. doi: 10.1115/detc2011-47772.
- [11] Ying Chen, Hua Li, Kai Jin, and Qing Song. Wind farm layout optimization using genetic algorithm with different hub height wind turbines. *Energy Conversion and Management*, 70:56–65, Jun 2013. ISSN 0196-8904. doi: 10.1016/j.enconman.2013.02.007.

- [12] Souma Chowdhury, Achille Messac, Jie Zhang, Luciano Castillo, and Jose Lebron. Optimizing the unrestricted placement of turbines of differing rotor diameters in a wind farm for maximum power generation. *Volume 1: 36th Design Automation Conference, Parts A and B*, Jan 2010. doi: 10.1115/detc2010-29129.
- [13] Souma Chowdhury, Jie Zhang, Achille Messac, and Luciano Castillo. Unrestricted wind farm layout optimization (uwflo): Investigating key factors influencing the maximum power generation. *Renewable Energy*, 38(1):16–30, Feb 2012. ISSN 0960-1481. doi: 10.1016/j.renene.2011.06.033.
- [14] Souma Chowdhury, Jie Zhang, Achille Messac, and Luciano Castillo. Optimizing the arrangement and the selection of turbines for wind farms subject to varying wind conditions. *Renewable Energy*, 52:273–282, Apr 2013. ISSN 0960-1481. doi: 10.1016/j.renene.2012.10.017.
- [15] Bryony L. Du Pont and Jonathan Cagan. An extended pattern search approach to wind farm layout optimization. *Volume 1: 36th Design Automation Conference, Parts A and B*, Jan 2010. doi: 10.1115/detc2010-28748.
- [16] Bryony DuPont, Jonathan Cagan, and Patrick Moriarty. An advanced modeling system for optimization of wind farm layout and wind turbine sizing using a multi-level extended pattern search algorithm. *Energy*, 106:802–814, Jul 2016. ISSN 0360-5442. doi: 10.1016/j.energy.2015.12.033.
- [17] Bryony L. DuPont, Jonathan Cagan, and Patrick Moriarty. Optimization of wind farm layout and wind turbine geometry using a multi-level extended pattern search algorithm that accounts for variation in wind shear profile shape. *Volume 3: 38th Design Automation Conference, Parts A and B*, Aug 2012. doi: 10.1115/detc2012-70290.
- [18] Christopher Elkinton, James Manwell, and Jon McGowan. Offshore wind farm layout optimization (owflo) project: Preliminary results. *44th AIAA Aerospace Sciences Meeting and Exhibit*, Jan 2006. doi: 10.2514/6.2006-998.
- [19] Yunus Eroğlu and Serap Ulusam Seçkiner. Design of wind farm layout using ant colony algorithm. *Renewable Energy*, 44:53–62, Aug 2012. ISSN 0960-1481. doi: 10.1016/j.renene.2011.12.013.
- [20] Yunus Eroğlu and Serap Ulusam Seçkiner. Wind farm layout optimization using particle filtering approach. *Renewable Energy*, 58:95–107, Oct 2013. ISSN 0960-1481. doi: 10.1016/j.renene.2013.02.019.
- [21] Fraunhofer Institute for Solar Energy Systems ISE. Levelized cost of electricity - renewable energy technologies, Jun 2021.
- [22] Sten Frandsen. On the wind speed reduction in the center of large clusters of wind turbines. *Journal of Wind Engineering and Industrial Aerodynamics*, 39(1-3):251–265, Jan 1992. ISSN 0167-6105. doi: 10.1016/0167-6105(92)90551-k.

- [23] Sebastian Gatscha. Generic optimization of a wind farm layout using a genetic algorithm. Master's thesis, University of Natural Resources and Life Science, Vienna, 2016.
- [24] S.A. Grady, M.Y. Hussaini, and M.M. Abdullah. Placement of wind turbines using genetic algorithms. *Renewable Energy*, 30(2):259–270, Feb 2005. ISSN 0960-1481. doi: 10.1016/j.renene.2004.05.007.
- [25] Huajie Gu and Jun Wang. Irregular-shape wind farm micro-siting optimization. *Energy*, 57:535–544, Aug 2013. ISSN 0360-5442. doi: 10.1016/j.energy.2013.05.066.
- [26] Tuhfe Göçmen, Paul van der Laan, Pierre-Elouan Réthoré, Alfredo Peña Diaz, Gunner Chr. Larsen, and Søren Ott. Wind turbine wake models developed at the technical university of denmark: A review. *Renewable and Sustainable Energy Reviews*, 60:752–769, Jul 2016. ISSN 1364-0321. doi: 10.1016/j.rser.2016.01.113.
- [27] Dr. Ing. Thomas Hahm. Turbulente Windparkplanung. *Erneuerbare Energien*, pages 118–123, September 2010.
- [28] Gregor Heiming. Modeling and simulation of offshore wind farms. Bachelor's thesis, RWTH Aachen University, 2015.
- [29] José Herbert-Acero, Oliver Probst, Pierre-Elouan Réthoré, Gunner Larsen, and Krystel Castillo-Villar. A review of methodological approaches for the design and optimization of wind farms. *Energies*, 7(11):6930–7016, Oct 2014. ISSN 1996-1073. doi: 10.3390/en7116930.
- [30] Peng Hou, Weihao Hu, Cong Chen, Mohsen Soltani, and Zhe Chen. Optimization of offshore wind farm layout in restricted zones. *Energy*, 113:487–496, Oct 2016. ISSN 0360-5442. doi: 10.1016/j.energy.2016.07.062.
- [31] Carlos M. Ituarte-Villarreal and Jose F. Espiritu. Optimization of wind turbine placement using a viral based optimization algorithm. *Procedia Computer Science*, 6:469–474, 2011. ISSN 1877-0509. doi: 10.1016/j.procs.2011.08.087.
- [32] Niels Otto Jensen. *A note on wind generator interaction*. Number 2411 in Risø-M. Risø National Laboratory, 1983. ISBN 87-550-0971-9.
- [33] I. Katic, J. Højstrup, and N.O. Jensen. A simple model for cluster efficiency. In W. Palz and E. Sesto, editors, *EWEC'86. Proceedings. Vol. 1*, pages 407–410. A. Raguzzi, 1987. European Wind Energy Association Conference and Exhibition, EWEC '86 ; Conference date: 06-10-1986 Through 08-10-1986.
- [34] Majid Khanali, Shahrzad Ahmadzadegan, Mahmoud Omid, Forough Keyhani Nasab, and Kwok Wing Chau. Optimizing layout of wind farm turbines using genetic algorithms in tehran province, iran. *International Journal of Energy*

- and Environmental Engineering*, 9(4):399–411, Jul 2018. ISSN 2251-6832. doi: 10.1007/s40095-018-0280-x.
- [35] Manfred Kleemann and Michael Meliß. *Regenerative Energiequellen*. Springer-Verlag, 2013.
- [36] Huan Long and Zijun Zhang. A two-echelon wind farm layout planning model. *IEEE Transactions on Sustainable Energy*, 6(3):863–871, Jul 2015. ISSN 1949-3037. doi: 10.1109/tste.2015.2415037.
- [37] Longfu Luo, Xiaofeng Zhang, Dongran Song, Weiyi Tang, Li Li, and Xiaoyu Tian. Minimizing the energy cost of offshore wind farms by simultaneously optimizing wind turbines and their layout. *Applied Sciences*, 9(5):835, Feb 2019. ISSN 2076-3417. doi: 10.3390/app9050835.
- [38] Grigorios Marmidis, Stavros Lazarou, and Eleftheria Pyrgioti. Optimal placement of wind turbines in a wind park using monte carlo simulation. *Renewable Energy*, 33(7):1455–1460, Jul 2008. ISSN 0960-1481. doi: 10.1016/j.renene.2007.09.004.
- [39] C. BalaKrishna Moorthy, M.K. Deshmukh, and Darshana Mukherejee. New approach for placing wind turbines in a wind farm using genetic algorithm. *Wind Engineering*, 38(6):633–642, Dec 2014. ISSN 2048-402X. doi: 10.1260/0309-524x.38.6.633.
- [40] Ivan Mustakerov and Daniela Borissova. Wind turbines type and number choice using combinatorial optimization. *Renewable Energy*, 35(9):1887–1894, Sep 2010. ISSN 0960-1481. doi: 10.1016/j.renene.2009.12.012.
- [41] Antonio Neiva, Vanessa Guedes, Caio Leandro Suzano Massa, and Daniel Davy Bello de Freitas. A review of wind turbine wake models for wind park optimization. *Proceedings of the 25th International Congress of Mechanical Engineering*, 2019. doi: 10.26678/abcm.cobem2019.cob2019-1109.
- [42] A. S. O. Ogunjuyigbe, T. R. Ayodele, and O. D. Bamgboje. Optimal placement of wind turbines within a wind farm considering multi-directional wind speed using two-stage genetic algorithm. *Frontiers in Energy*, 15(1):240–255, Dec 2017. ISSN 2095-1698. doi: 10.1007/s11708-018-0514-x.
- [43] Leandro Parada, Carlos Herrera, Paulo Flores, and Victor Parada. Wind farm layout optimization using a gaussian-based wake model. *Renewable Energy*, 107: 531–541, Jul 2017. ISSN 0960-1481. doi: 10.1016/j.renene.2017.02.017.
- [44] Jeong Woo Park, Bo Sung An, Yoon Seung Lee, Hyunsuk Jung, and Ikjin Lee. Wind farm layout optimization using genetic algorithm and its application to daegwallyeong wind farm. *JMST Advances*, 1(4):249–257, Nov 2019. ISSN 2524-7913. doi: 10.1007/s42791-019-00026-z.

- [45] Jaydeep Patel, Vimal Savsani, Vivek Patel, and Rajesh Patel. Layout optimization of a wind farm to maximize the power output using enhanced teaching learning based optimization technique. *Journal of Cleaner Production*, 158:81–94, Aug 2017. ISSN 0959-6526. doi: 10.1016/j.jclepro.2017.04.132.
- [46] Alfredo Peña, Pierre-Elouan Réthoré, and Ole Rathmann. Modeling large offshore wind farms under different atmospheric stability regimes with the park wake model. *Renewable Energy*, 70:164–171, Oct 2014. ISSN 0960-1481. doi: 10.1016/j.renene.2014.02.019.
- [47] S. Rodrigues, P. Bauer, and Peter A.N. Bosman. Multi-objective optimization of wind farm layouts - complexity, constraint handling and scalability. *Renewable and Sustainable Energy Reviews*, 65:587–609, Nov 2016. ISSN 1364-0321. doi: 10.1016/j.rser.2016.07.021.
- [48] Michele Samorani. *The Wind Farm Layout Optimization Problem*. Springer Berlin Heidelberg, 2013. ISBN 9783642410802. doi: 10.1007/978-3-642-41080-2\_2.
- [49] Peter Sanderhoff. *PARK- User’s Guide. A PC-program for calculation of wind turbine park performance*. Number 668(EN) in Risø-I. Risø National Laboratory, Jan 1993.
- [50] M. S. Selig and V. L. Coverstone-Carroll. Application of a genetic algorithm to wind turbine design. *Journal of Energy Resources Technology*, 118(1):22–28, Mar 1996. ISSN 1528-8994. doi: 10.1115/1.2792688.
- [51] Javier Serrano González, Manuel Burgos Payán, Jesús Manuel Riquelme Santos, and Francisco González-Longatt. A review and recent developments in the optimal wind-turbine micro-siting problem. *Renewable and Sustainable Energy Reviews*, 30:133–144, Feb 2014. ISSN 1364-0321. doi: 10.1016/j.rser.2013.09.027.
- [52] Rabia Shakoor, Mohammad Yusri Hassan, Abdur Raheem, and Yuan-Kang Wu. Wake effect modeling: A review of wind farm layout optimization using Jensen’s model. *Renewable and Sustainable Energy Reviews*, 58:1048–1059, May 2016. ISSN 1364-0321. doi: 10.1016/j.rser.2015.12.229.
- [53] Joongjin Shin, Seokheum Baek, and Youngwoo Rhee. Wind farm layout optimization using a metamodel and ea/pso algorithm in Korea offshore. *Energies*, 14(1): 146, Dec 2020. ISSN 1996-1073. doi: 10.3390/en14010146.
- [54] Dongran Song, Xinyu Fan, Jian Yang, Anfeng Liu, Sifan Chen, and Young Hoon Joo. Power extraction efficiency optimization of horizontal-axis wind turbines through optimizing control parameters of yaw control systems using an intelligent method. *Applied Energy*, 224:267–279, Aug 2018. ISSN 0306-2619. doi: 10.1016/j.apenergy.2018.04.114.

- [55] Thomas Sørensen, Per Nielsen, and Morten Lybech Thøgersen. Recalibrating wind turbine wake model parameters - validating the wake model performance for large offshore wind farms, 2006.
- [56] Ahmadreza Vassel-Be-Hagh and Cristina L. Archer. Wind farm hub height optimization. *Applied Energy*, 195:905–921, Jun 2017. ISSN 0306-2619. doi: 10.1016/j.apenergy.2017.03.089.
- [57] Feng Wang, Deyou Liu, and Lihua Zeng. Study on computational grids in placement of wind turbines using genetic algorithm. *2009 World Non-Grid-Connected Wind Power and Energy Conference*, Sep 2009. doi: 10.1109/wnwec.2009.5335776.
- [58] Robert Whittlesey. Vertical axis wind turbines. *Wind Energy Engineering*, pages 185–202, 2017. doi: 10.1016/b978-0-12-809451-8.00010-2.
- [59] Yin yin Lo. Multi-step layout-optimization of turbines in offshore wind farms. Bachelor’s thesis, RWTH Aachen University, 2020.